

Coastal Forests as a Tsunami Mitigation Measure
in Pacific Northwest Coastal Communities

Brook A Goodwin

A thesis

submitted in partial fulfillment of the
requirements for the degrees of

Master of Landscape Architecture

Master of Urban Planning

University of Washington

2022

Committee:

Kenneth P. Yocom

Daniel B. Abramson

Programs Authorized to Offer Degrees:

Landscape Architecture

Urban Design & Planning

©Copyright 2022
Brook A Goodwin

University of Washington

Abstract

Coastal Forests as a Tsunami Mitigation Measure
in Pacific Northwest Coastal Communities

Brook A Goodwin

Co-Chairs of the Supervisory Committee:

Kenneth P. Yocom

Landscape Architecture

Daniel B. Abramson

Urban Design & Planning

The Pacific Northwest coast has tsunami risk in both non-local and local forms. Most significant is the tsunami risk that comes from the Cascadia subduction zone, and scientists predict that more major seismic events along this zone are due to occur in the future. These events may generate tsunami waves in excess of 30 feet for PNW coasts, leaving coastline areas with as little as 15 minutes advance warning to prepare and seek high ground shelter. Given this significant risk of non-local and local tsunamis, multiple tsunami mitigation measures and emergency preparedness strategies have been implemented in Washington's coastal communities.

It was learned from the 2011 Great East Japan Tsunami that coastal forests were not negligible in mitigation of the tsunami. In this design research thesis, I explore the applications of coastal forests as a natural tsunami mitigation measure in PNW coastal communities. Specifically, there are two research questions I investigate: 1) What elements of a coastal forest contribute to effective tsunami mitigation? and 2) How can these elements be translated into a coastal forest design to function as a

tsunami mitigation measure?

Coastal forests have clear potential for tsunami mitigation. When designed with the five Performance Factors in mind (forest area, gap layering, tree crown height, tree distribution, landform), they can have direct effects on a tsunami's wave energy, flow speed, inundation depth, and inundation extent. This mitigation potential can result in positive changes to tsunami risk by slowing wave inundation rates and increasing evacuation warning times. This site-specific design investigation in Westport, WA could influence future site developments to include coastal forests for tsunami mitigation purposes. Further research on the properties of coastal forests that can contribute to tsunami mitigation need to be carried out in the fields of soils and geoengineering, forest restoration, park and campground site design, and ecotourism and economic development.

Acknowledgments

I would like to thank my thesis committee co-chairs Ken Yocom and Dan Abramson for their guidance and advice in the creation of this document. I would also like to thank Julie Parrett and Diana Siembor for all of their curriculum and administrative advice in the MLA-MUP Concurrent Degree Program.

I truly appreciate my partner, family, and all my friends who supported me through these four years of graduate study. I could not have done it without you all!

Contents

Figures.....	viii
Tables.....	xi
Introduction	
Framing the Issue	1
<i>What is a tsunami?</i>	1
<i>Tsunami Risk for Pacific Northwest Coast</i>	5
<i>Types of Mitigation Measures</i>	7
<i>Scientific Background</i>	10
Research Problem.....	11
Purpose Statement.....	12
Literature Review	
Mitigating Elements of Coastal Forests	13
<i>Aspect Ratio</i>	14
<i>Single- and Double-Layered Models</i>	15
<i>Crown Height</i>	16
<i>Tree Distribution</i>	17
<i>Landform</i>	18
Performance Factors	
Forest Area.....	20
Gap Layering	21
Tree Crown Height	21
Tree Distribution.....	22
Landform.....	24
Effects of Factors	24
Case Studies	
Coastal Forest Restoration – Natori, Japan	25
Tsunami Mitigation Parks – Japan, Indonesia, Chile	26

Application to the Pacific Northwest	
Suitability Criteria	29
Westport Tsunami Risk	32
Existing Measures	35
Site Analysis	35
<i>Soils</i>	41
<i>Topography</i>	42
<i>Plant Inventory</i>	43
Design Investigation	
Tree Selection	45
Five Tree Species	47
Understory Plantings	48
Tree Distribution	49
Landform	51
Phasing	51
Discussion – Conclusion	
Tsunami Mitigation Potential	53
Changes to Tsunami Risk	53
Influence on Future Site Developments	54
Further Research	55
References	56

Figures

1. A tsunami wave overtaking a seawall in Japan in 2011.....	1
2. Map showing the epicenter of the earthquake and the severity levels felt on the mainland.....	2
3. Waves from the tsunami crash over the sea wall in Miyako, Japan.	3
4. Debris was washed ashore by the tsunami.....	3
5. Members of the Japanese Ground Self-Defense Force in search and rescue operations.....	3
6. Tsunami waves crash through coastal trees.....	3
7. Large tsunami waves rush inland.	3
8. Large-scale flooding from tsunami.....	3
9. Location of Tonga.....	4
10. Satellite image of the eruption.....	4
11. Some boats and debris washed ashore in Tonga.....	4
12. A tsunami wave rushing across the shore in Tonga.	4
13. Heat map of GEJT wave amplitudes across the Pacific Ocean, based on NOAA modeling.	5
14. Cascadia subduction zone location.....	6
15. A large sea wall with some armament behind it.....	7
16. A large sea wall being constructed.	7
17. A bus drives along a road next to a sea wall.	7
18. A beach armament installation made of large rock rip-rap in Tauranga, New Zealand.	8
19. Beach armament made of heaps of large boulders in the UK.	8
20. A tsunami warning siren in Edmonds, WA.....	8
21. Rendering of a new tsunami evacuation tower for the Shoalwater Bay Tribe.	9
22. The first vertical tsunami evacuation structure in the Ocosta School District.....	9
23. An architectural rendering showing the evacuation structure.	9
24. A coastal forest in Oregon.....	10
25. A coastal forest in northern Washington.	10
26. Diagram showing studies read during the initial lit review	13
27. Diagram showing relationship between composition elements and types of mitigation.	14

28. Diagram showing aspect ratio as a relationship between forest length and width.	20
29. Diagram showing forest layout with alternating gaps.	21
30. Diagram showing the relationship of overall tree height to crown height.....	22
31. Diagram showing seaward species and landward species placement.....	23
32. Diagram showing forest layout with alternating gaps.	24
33. A before and after image of Natori City and its forest.	25
34. A ground-level photo of the toppled forest.	25
35. Japanese black pine seedlings are grown in a nursery	25
36. Aerial photo of the forest restoration area.....	25
37. A rendering that shows a hybrid mitigation park layout with a coastal forest and sea wall.....	26
38. A recently planted section of forest in the Morino Project.....	26
39. Forest restoration work being performed by community volunteers in the Morino Project.	27
40. A section of recently planted seedlings in the Morino Project.	27
41. The President of Indonesia visiting mangrove replanting efforts.....	27
42. Aerial photo showing the shoreline of Constitución, Chile.	28
43. A before and after rendering of one of the forested park areas in Constitución, Chile.....	28
44. Context map showing location of Grays Harbor in Washington.	29
45. Westport Golf Links land use and site analysis map.	31
46. Map showing tsunami inundation depths for Westport, WA.	32
47. Map showing tsunami inundation speeds for Westport, WA.	33
48. Map showing evacuation walk times for Westport, WA.	34
49. Rock wall beach armaments along the northern coast of Westport.	35
50. Context map showing the location of Westport Light State Park.	36
51. Pacific shoreline of Westport Light State Park.....	37
52. Half Moon Bay on the northern edge of Westport Light State Park.	37
53. Walking path along the dune in Westport Light State Park.	37
54. Restroom building at the northwestern corner of Westport Light State Park.....	37
55. Map showing the areas of shoreline, dune, shrubland, and forest.....	38
56. Ocean shoreline and foredune.....	39
57. Dune plain and walking path.....	39

58. Backdune and shrubs.	39
59. Shrubland and forest.	39
60. Forest area near the lighthouse.....	39
61. Map showing the study area within the park.....	40
62. Color-coded 5-foot contour map	43
63. USDA MLRA map showing Sitka Spruce Belt in Grays Harbor, WA.....	45
64. Image collage of the proposed trees.	46
65. Diagram showing tree species distribution within the proposed forest area.....	50
66. Section A showing the topography of a southern section of the site, facing north.....	51
67. Phasing diagram showing how the phases relate to one another along a timeline.	51
68. Map showing the potential area for coastal forest development within golf course.....	55

Tables

1. Matrix showing a comparison of Ocean Shores and Westport.....	30
2. Planting palette showing existing foredune and backdune plant species.....	44
3. Planting palette showing existing dune plain and forest plant species.....	44
4. Proposed tree schedule with details for each of the five trees.....	46
5. Planting palette showing proposed understory plant species.....	48
6. Proposed understory plant schedule with details for each species.....	48

Introduction

In this design research thesis, I explore the applications of coastal forests as a natural tsunami mitigation measure in Pacific Northwest (PNW) coastal communities. Specifically, there are two research questions I investigate: 1) What elements of a coastal forest contribute to effective tsunami mitigation? and 2) How can these elements be translated into a coastal forest design to function as a tsunami mitigation measure?

Framing the Issue

What is a tsunami?

As described by the National Oceanic and Atmospheric Administration (NOAA), a tsunami is a series of extremely long waves, caused by a large and sudden displacement of water. This displacement is most commonly caused by earthquakes, but can also result from volcanic eruptions, large underwater landslides, and meteorite impacts. These waves can move across entire ocean basins. Once reaching a coastline, they can cause dangerous coastal flooding and powerful currents, lasting for several hours or even days. The waves appear not as a “tidal wave” but as a rapidly-rising flood (see fig. 1). Tsunamis can be both local (or generated nearby) and non-local (or trans-oceanic). Globally, local tsunamis occur approximately twice per year, and tsunamis large enough to have non-local effects occur approximately twice per decade (“Tsunami Frequently Asked Questions” n.d.).



Figure 1. A tsunami wave overtaking a seawall in Japan in 2011. Photo by Mainichi Shimbun/Reuters (Shimbun 2021).

Two recent examples of tsunamis are the 2011 Great East Japan Tsunami (GEJT) and the 2022 Hunga Tonga–Hunga Ha’apai eruption and tsunami. The GEJT occurred off the western coast of Japan and was one of the most impactful tsunamis on record. It was caused by a Magnitude 9.1 earthquake and resulted in a massive local tsunami with waves of over 30 feet and massive amounts of water rushing inland. Dozens of coastal cities suffered widespread flooding, severe structural damage, and thousands of deaths (see fig. 2) (“On This Day: 2011 Tohoku Earthquake and Tsunami” 2021). The flooding from the tsunami also damaged the Fukushima Daiichi Nuclear Power Plant, considered the most severe nuclear accident since Chernobyl (see fig. 3 – 8) (McCurry 2011). Non-local trans-Pacific tsunami waves were also recorded at coastal sea level gauges in over 25 Pacific Rim countries including the US. Over \$31 million of damage in Hawaii and \$100 million in damages to marine facilities in California were reported. Luckily, only two deaths outside of Japan occurred. (“On This Day: 2011 Tohoku Earthquake and Tsunami” 2021).



Figure 2. Map showing the epicenter of the earthquake and the severity levels felt on the mainland. Map by Encyclopedia Britannica (*Japan Earthquake of 2011* n.d.).



Figure 3. Waves from the tsunami crash over the sea wall in Miyako, Japan. Photo by Miyako City Officer/Shutterstock.com via Encyclopedia Britannica (*Japan Earthquake and Tsunami of 2011* 2011).



Figure 4. Debris was washed ashore by the tsunami. Photo by Petty Officer 1st Class Matthew Bradley/U.S. Navy via Encyclopedia Britannica (*Wreckage From Japan Earthquake and Tsunami of 2011* 2011).



Figure 5. Members of the Japanese Ground Self-Defense Force in search and rescue operations in Ofunato, Japan. Photo by Matt Dunham—AP/Shutterstock.com via Encyclopedia Britannica (*Japanese Ground Self-Defense Force, Ofunato, Iwate prefecture, Japan 2011*).



Figure 6. Tsunami waves crash through coastal trees. Photo by Sadatsugu Tomizawa/AFP via Getty Images (Tomizawa 2011).



Figure 7. Large tsunami waves rush inland. Photo by Kyodo/Reuters (*When the Japan Tsunami Struck 2011a*).



Figure 8. Large-scale flooding from tsunami. Photo by Kyodo/Reuters (*When the Japan Tsunami Struck 2011b*).

The 2022 Hunga Tonga–Hunga Ha’apai eruption and tsunami is the most recent significant tsunami event at the time of this writing. This tsunami was caused by the explosive eruption of an underwater volcano, called Hunga Tonga–Hunga Ha’apai, part of the Polynesian archipelago country of Tonga in the south Pacific (see fig. 9) (“Tonga Volcanic Eruption and Tsunami, January 15, 2022” 2022). This explosion threw a volcanic ash cloud more than 12 miles into the atmosphere and generated a massive atmospheric shockwave that traveled across the Pacific Ocean (see fig. 10) (Sharma and Scarr 2022). A small tsunami up to just under 4 feet occurred that flooded coastal areas in Tonga (see fig. 11 and 12). Across the Pacific, water level changes resulting from the tsunami were recorded in Tonga, Vanuatu, New Caledonia, Australia, Cook Islands, New Zealand, Hawaii, Japan, Chile, Alaska, and California. Deaths were reported in Tonga and Peru (“Tonga Volcanic Eruption and Tsunami, January 15, 2022” 2022).



Figure 9. Location of Tonga. Map by The New York Times (*Mapping a First Look at Tonga’s Devastation After the Volcano Eruption 2022*).

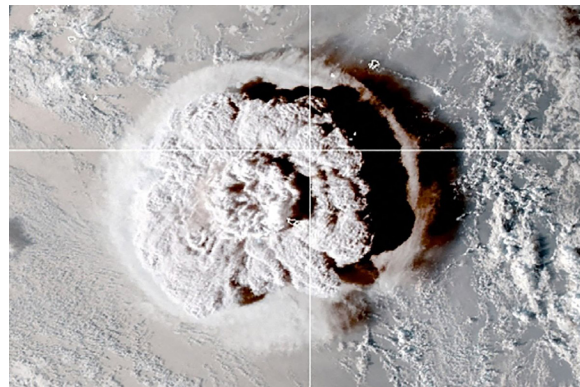


Figure 10. Satellite image of the eruption. Image by CIRA/NOAA via Reuters (*Tsunami Models Underestimated Shockwave from Tonga Eruption 2022a*).



Figure 11. Some boats and debris washed ashore in Tonga. Photo by Malau Media/Reuters (*Tsunami Models Underestimated Shockwave from Tonga Eruption 2022b*).



Figure 12. A tsunami wave rushing across the shore in Tonga. Photo by Faka’iloatonga Taumoefolau @sakakimoana/Twitter via CNN (*Taumoefolau 2022*).

Tsunami Risk for Pacific Northwest Coast

The PNW coast has tsunami risk in both non-local and local forms. Non-local tsunami risk includes all trans-Pacific tsunami events. These very large waves are transmitted long distances over the ocean and increase in amplitude as they approach the coastlines. At first these tsunamis are usually realized as small waves of 10 feet or less in deep water but increase rapidly in amplitude as they approach the coastlines (“Tsunami Frequently Asked Questions” n.d.). Figure 13 shows how the large waves from this tsunami were transmitted across the Pacific Ocean.

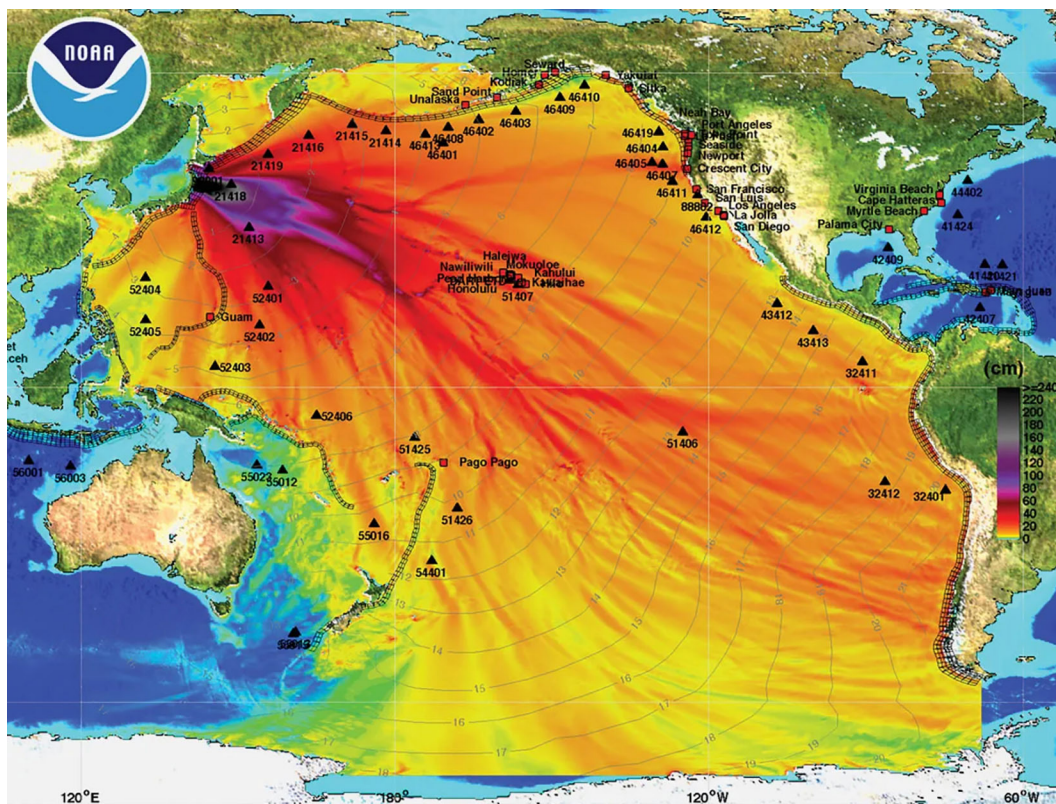


Figure 13. Heat map of GEJT wave amplitudes across the Pacific Ocean, based on NOAA modeling. Map by NOAA via Encyclopedia Britannica (*Tsunami Wave Height Model* 2011).

Local tsunami risk comes from the Cascadia subduction zone (CSZ). This is a major subduction zone about 700 miles long and located in the Pacific Ocean approximately 70 – 100 miles off the coast of Vancouver Island, Washington, Oregon, and Northern California (see fig. 14) (“JetStream Max: Cascadia Subduction Zone” 2019). Geological studies and records indicate that historical seismic events originating from the CSZ resulted in multiple local tsunamis in the past along the PNW coast (Walton et al. 2021). Scientists predict that more major seismic events along this zone are due to

occur in the future (Witter et al. 2013). These events may generate large earthquakes of magnitude 8 or 9 and tsunami waves in excess of 30 feet for PNW coasts, leaving coastline areas with as little as 15 minutes advance warning to prepare and seek high ground shelter (“JetStream Max: Cascadia Subduction Zone” 2019). Given this significant risk of non-local and local tsunamis, multiple tsunami mitigation measures and emergency preparedness strategies have been implemented in Washington’s coastal communities (“Preparation and Evacuation” n.d.; “Tsunami” n.d.).



Figure 14. Cascadia subduction zone location. Map by Alicia Iverson, distributed under CC BY-SA 4.0 license via Wikimedia Commons (Iverson 2015).

Types of Mitigation Measures

Various types of artificial and natural mitigation measures exist to reduce the wave forces and inundation extents of tsunamis, or to get people out of harm's way. The most common of the artificial measures include sea walls, beach armaments, warning sirens, vertical evacuation towers, and horizontal evacuation routes. Natural mitigation measures such as vegetation and landform can be found in coastal dunes and forests.

Sea walls are typically large concrete structures that are specifically engineered to withstand tsunami wave forces and hold back the rising waters. They are effective as long as the tsunami wave height does not exceed the wall height. Sea walls vary in height from a few to dozens of feet. Currently, the largest sea walls are being built along the western coast of Japan as a response to the 2011 GEJT. These walls span around 245 miles of coastline and exceed 40 feet in height in some areas (see fig. 15 – 17) (Kyung-Hoon 2018d).



Figure 15. A large sea wall with some armament behind it. Photo by Kim Kyung-Hoon/Reuters (Kyung-Hoon 2018c).



Figure 16. A large sea wall being constructed. Photo by Kim Kyung-Hoon/Reuters (Kyung-Hoon 2018b).

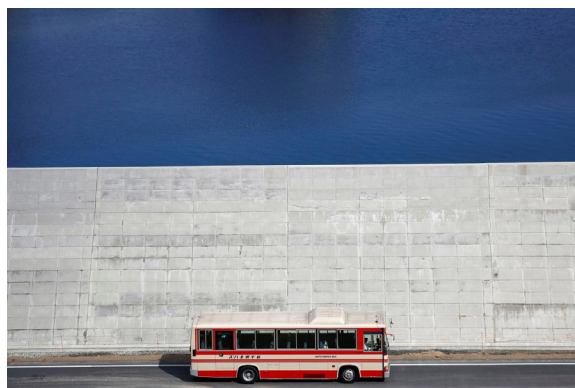


Figure 17. A bus drives along a road next to a sea wall. Photo by Kim Kyung-Hoon/Reuters (Kyung-Hoon 2018a).

Beach armaments are assemblages of concrete rubble, boulders, and other large objects that are strategically located along coastline water edges. Their primary purpose is to prevent beach erosion from normal wave action and to hold back high tide waters. Beach armaments can also be effective in small tsunamis by reducing the wave force and holding back some of the rising water. However, a larger tsunami may easily overtop or destroy them (see fig. 18 and 19) (“Resource Issues: Coastal Armoring and Erosion” 2019).



Figure 18. A beach armament installation made of large rock rip-rap in Tauranga, New Zealand. Photo by Cirtex Industries (*Tauranga Sea Wall Rock Revetment – TerraTex K Geotextile* 2018).



Figure 19. Beach armament made of heaps of large boulders in the UK. Photo distributed under CC BY 2.5 license via PhotoEverywhere.co.uk (*Sea Wall Coastal Defense* 2008).

Warning sirens are multidirectional loudspeakers that are connected to special sensors in the Pacific Ocean as part of an early warning system. The sensors can detect changes in the ocean indicative of an incoming tsunami and trigger the early warning system. The sirens emit a loud tone that can be heard across long distances, alerting people nearby of the tsunami warning and advising them to prepare and seek high ground shelter. Sirens like these are distributed in coastal areas such as western Washington (see fig. 20) (“U.S. Tsunami Warning System” 2016). The siren system, also known as an All-Hazards Alert Broadcast or AHAB, includes more than 70 sirens along the Washington coast (Buehner 2021).



Figure 20. A tsunami warning siren in Edmonds, WA. Photo by Everett Post (*Outdoor Tsunami Warning Sirens Coming to the North Sound* 2021).

Vertical evacuation structures are tall towers, berms, or other structures that are specifically designed to withstand the wave forces of a tsunami. The towers can provide safe high ground for hundreds of people above the flood waters. Towers can be stand-alone structures (see fig. 21) or integrated into another building. One example of an integrated tower is the Ocosta School building in Westport, WA (see fig. 22). This building was designed as a gymnasium with four staircases on each corner that lead to the roof. The staircases and the roof function as a tsunami evacuation tower and can hold up to 700 people (see fig. 23). The exterior entry doors of the staircases are connected to the early warning system and will automatically unlock if a tsunami warning is issued. This building was completed in 2016 and is the first of its kind in the United States (“Project Safe Haven: Tsunami Vertical Evacuation Systems on Washington State’s Pacific Coast” 2021).



Figure 21. Rendering of a new tsunami evacuation tower for the Shoalwater Bay Tribe near Tokeland, WA. Image by Visual Engineering Resource Group via Chinook Observer (*Design Work Underway for Shoalwater Tsunami Evacuation Tower* 2019).



Figure 22. The first vertical tsunami evacuation structure was built as part of a new elementary school in the Ocosta School District in Westport, WA. Photo via WA DNR (*Tsunamis / Preparation and Evacuation / Vertical Evacuation* n.d.-a).

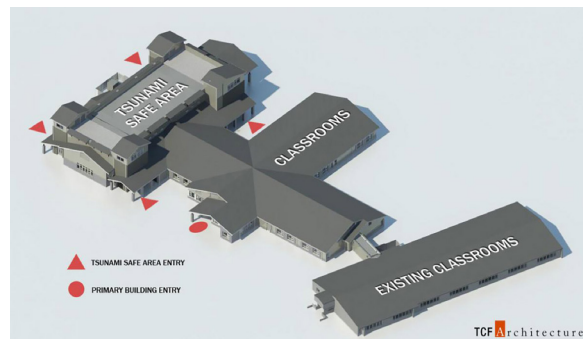


Figure 23. An architectural rendering showing the layout of the buildings and the evacuation structure. Image by TCF Architecture via WA DNR (*Tsunamis / Preparation and Evacuation / Vertical Evacuation* n.d.-b).

Coastal forests include vegetation and landform that can potentially serve as a natural mitigation measure for tsunamis. Coastal forests can be complementary to other artificial measures, reducing the wave force, flow speed, and inundation extent. Additionally, coastal forests can provide human-friendly beachfronts, forest and coastal habitat restoration, and economic and recreational benefits such as ecotourism (see fig. 24 and 25) (Tanaka, 2009).



Figure 24. A coastal forest in Oregon. Photo by Sue/ ExplorerSue.com (Sue 2017).



Figure 25. A coastal forest in northern Washington. Photo by John Callery via Dreamstime.com (Callery n.d.).

Scientific Background

Since the mid-1980s, scientists and researchers have been uncovering geological evidence of historic local tsunamis along the PNW coast. Studies of global subduction zones (Heaton and Kanamori 1984; Heaton and Hartzell 1986; 1989) led to the recognition of potential for seismic events and associated tsunamis along the CSZ off the Pacific coast. Paleoseismologic studies have focused on the last large geologic event in 1700 CE (Atwater 1987; 1992; Atwater and Hemphill-Haley 1997; Kelsey et al. 2002; Witter et al. 2003). Analysis of tsunami records in Japan independently corroborated the 1700 CE event, concluding that a non-local tsunami that struck Japan most likely came from a large earthquake along the CSZ (Satake et al. 1996; Satake et al. 2003). Additionally, geologic deposits along the Washington-Oregon transition zone from coastal to deep ocean seafloor show evidence of about 13 great Cascadia earthquakes (Adams 1996; Goldfinger et al. 2003). These range of studies suggest the potential for local tsunami events from the CSZ and the threat of tsunami inundation and disaster for PNW coastal communities.

The 2011 GEJT was one of the most impactful tsunamis on record and can be considered a case

study for comparable tsunami threat in the PNW. Multiple studies have been conducted on the performance of tsunami mitigation measures present during the GEJT. The GEJT exceeded the designed level of coastal defense and extensively destroyed parts of sea walls, tsunami gates, and large armaments (Tappin et al. 2012). There was catastrophic damage to people and buildings in the Tohoku and Kanto regions of Japan (Udo et al. 2012; Suppasri et al. 2013). Coastal forests were also destroyed (Tanaka et al. 2013).

Research Problem

It was learned from the GEJT that coastal forests were not negligible in mitigation of the tsunami (Tanaka et al. 2014). Even after trees are broken or overturned, the remaining forest still acts to mitigate the tsunami by trapping floating debris (Tanaka 2012; Pasha and Tanaka 2016). Previous studies also recognized the effectiveness of coastal vegetation for tsunami mitigation including post-disaster surveys after the 1998 Papua New Guinea tsunami (Dengler and Preuss 2003), 2004 Indian Ocean tsunami (Danielsen et al. 2005; Mascarenhas and Jayakumar 2008; Tanaka et al. 2007), and the GEJT (Nandasena et al. 2012; Tanaka 2012; Tanaka et al. 2014).

However, limitations of the tsunami mitigating ability of coastal forests have also been discussed. This includes the destruction of the coastal forest itself (Tanaka et al. 2007), the production of driftwood (Dengler and Preuss 2003; Cochard et al. 2008), flow channeling through gaps in a coastal forest (Thuy et al. 2009; Nandasena et al. 2012; Tanaka 2009; Samarakoon et al. 2013), and the formation of strong currents behind a forest (Iimura and Tanaka 2013). Both field surveys and physical experiments indicate the effectiveness of vegetation for tsunami mitigation (Irtem et al. 2009; Ismail et al. 2012).

In PNW coastal communities, much effort in tsunami mitigation is being developed as structural (hard) measures, such as sea walls, evacuation structures, and beach armament, and non-structural (soft) measures that are more programmatic or focused on building social resilience such as learned response strategies, public awareness campaigns, and evacuation planning (Suppasri et al. 2013). For structural measures, there are artificial methods like sea walls and natural methods like coastal

vegetation. Natural methods can be more effective in some ways than artificial methods alone, and they require comparatively little capital investment. They provide human-friendly beachfronts and can include many ecological, recreational, and economical benefits (Tanaka 2009).

Purpose Statement

In this design research thesis, I explore the applications of coastal forests as a natural tsunami mitigation measure in PNW coastal communities. Specifically, there are two research questions I investigate: 1) What elements of a coastal forest contribute to effective tsunami mitigation? and 2) How can these elements be translated into a coastal forest design to function as a tsunami mitigation measure?

Literature Review

Mitigating Elements of Coastal Forests

Many studies have been carried out on the physical and hydrological forces that are applied to coastal forests during a tsunami. Most of these studies involve laboratory testing and hydrological flow modeling to simulate the behavior of water when moving through or against stands of trees. The subjects of these studies include driftwood, tree breakage, and floating debris (Tanaka et al. 2014; 2018; Tanaka and Onai 2017; Tanaka and Ogino 2017; Iimura, Tanaka, and Ikeda 2013; Pasha and Tanaka 2016); sea embankment (Igarashi and Tanaka 2018); crown height (Anjum, Tanaka, and Rahman 2021); tree canopy and drag force (Nomura et al. 2021); rear current zone (Iimura and Tanaka 2013); run up (Irtem et al. 2009; Ismail, Abd Wahab, and Alias 2012); open gap (Thuy et al. 2009; Thuy, Tanimoto, and Tanaka 2010; Samarakoon, Tanaka, and Iimura 2013); sediment transport (Kusumoto et al. 2020); wave effect (Tognin et al. 2019; Tsai et al. 2017); sea walls (Nateghi et al. 2016); scouring (Ali and Tanaka 2020); and vegetation bioshields (Tanaka et al. 2009; Tanaka 2009). There was a wide span of research in tsunamis, coastal resiliency, and coastal forests discovered during the initial literature review (see fig. 26).

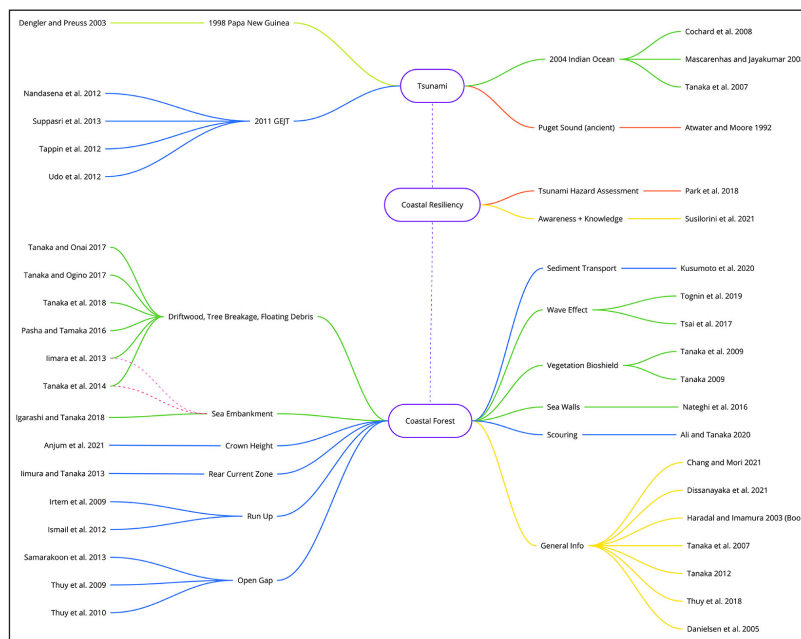


Figure 26. Diagram showing studies read during the initial lit review and the wide span of existing research in tsunamis and coastal forests. Image by Brook Goodwin (2021).

Various elements of a coastal forest’s composition contribute to different types of mitigation. These elements include tree breakage, crown height, trunk diameter, crown shape, tree types/species, distribution, aspect ratio, understory shrubs, landform and soil composition, and layering. Types of mitigation are drag force, debris trapping, scouring, adaptability, and gaps (see fig. 27). Five of these composition elements have been identified as the greatest contributors to mitigation and have been given a more in-depth literature review, as follows.

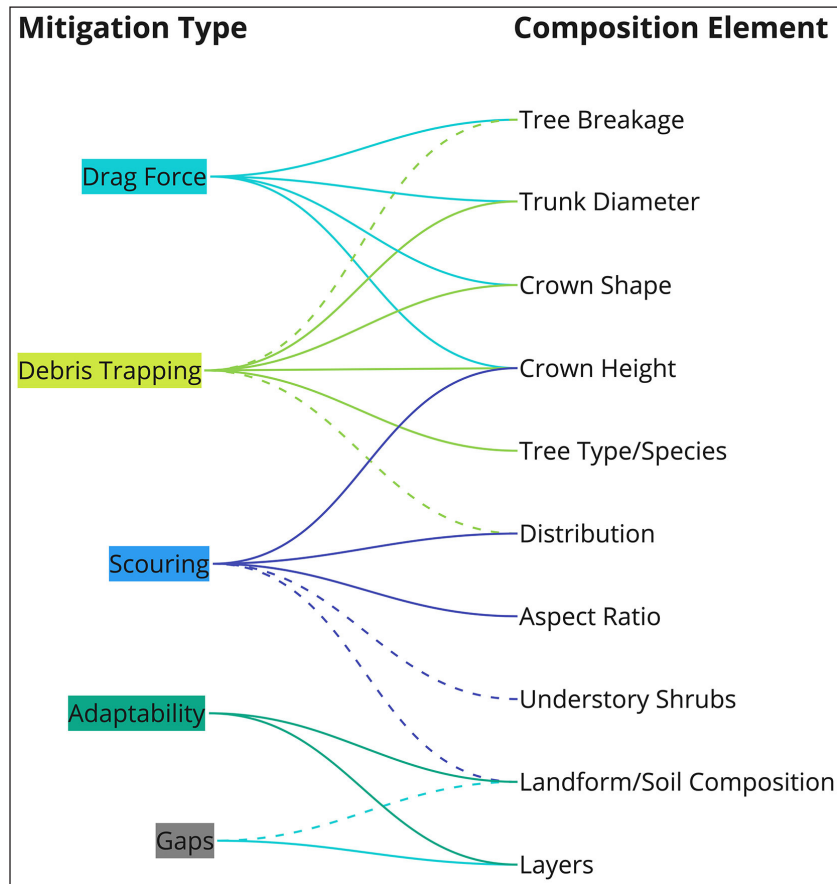


Figure 27. Diagram showing the relationship between composition elements of coastal forests and the types of mitigation they affect. Image by Brook Goodwin (2021).

Aspect Ratio

Limura and Tanaka (2013) considered how the width-length ratio (i.e. aspect ratio) of a span of coastal forest would affect tsunami mitigation. Previous research had focused on the density (Limura et al. 2011) and width (Tanimoto et al. 2007) of forests, but the length (i.e. parallel to the shoreline) was set at infinity or semi-infinity in many cases. Additionally, the flow velocity and tsunami force at the edge or exit of a gap had been verified (Thuy et al. 2009; 2010), but the effects

behind a short forest with a small aspect ratio had not been discussed yet.

Numerical simulations were used to evaluate bed resistance, drag, and turbulence-induced shear forces due to interaction with the forest. The results indicated that when a limited-length dense forest exists with an aspect ratio of 1 to 4, the tsunami at the edge of the forest diffracts and collides behind the forest with a fluid force that is larger than in a case where the forest does not exist. In similar forests with aspect ratios of greater than 4, the effects of this collision are reduced and overall lessened. Based on these results, it seems recommended that coastal forests be designed with an aspect ratio of 4 or greater in order to avoid creating a dangerous collision zone behind the forest.

Single- and Double-Layered Models

Tariq et al. (2021) measured and compared flow structures and loss of energy in three different vegetation structures: a single patch of finite length (i.e. parallel to shoreline), single- or double-layered with gaps, and continuous (i.e. full length) models. Previous research showed that an open gap in vegetation has a negative effect on tsunami run-up behind a forest (Mascarenhas and Jayakumar 2008). The study assessed whether double-layered vegetation models are more effective than single-layer, finite length, and continuous vegetation models. Water flume experiments were carried out to determine the flow properties under different vegetation conditions. Vegetation density (i.e. cylinders per square centimeter) and aspect ratio were the two primary parameters and greatly affected the flood flow behavior (Pasha and Tanaka 2020). The results showed that for a single patch model, an increase in the vegetation density and aspect ratio increased the backwater rise in front of the vegetation, reduced velocity, and enhanced energy dissipation. For single- and double-layered models, the loss of energy was higher in double-layered models, and gaps between patches in single-layered models had high flow velocities. The high velocities in these gaps could be countered by adding a second horizontal layer with an alternate gap.

Knowledge from this study could be applied in areas of a coastal forest where it is not possible to provide a continuous length of vegetation, such as around existing or necessary roads, pathways,

and structures. In such cases, a coastal forest should be designed as a series of patches with a smaller aspect ratio, but not of less than 4 as indicated in Iimura and Tanaka (2013) and alternating open gaps.

Crown Height

The effect of tree crown height on tsunami mitigation was investigated by Anjum et al. (2021). In previous studies (Irtem et al. 2009; Ismaili et al. 2012) using both physical and computational models, a simplified tree model in the form of a circular cylinder was used. The tree crown and its height from the ground has been shown to be significantly important in damage differences during a post-tsunami survey after the 2011 GEJT (Sato et al. 2012). Although some previous studies highlighted the importance of tree crowns in relation to breaking patterns (Tanaka et al. 2013; 2015; 2018), not many studies focused on differences of flow, scouring, or resistance due to changes in crown height. This study had three main objectives: 1) investigate the effects of tree crown height on tsunami mitigation and scour pattern under a movable gravel bed, 2) demonstrate flow structure changes and energy reduction between different forest densities and crown heights, and 3) develop and propose an effective bioshield against inland approaching tsunami currents. The ideal bioshield would withstand the impact of intense tsunami fluid forces and produce less driftwood due to scouring. They pursued these objectives using flume experiments under quasi-steady flow conditions, varying different parameters such as crown heights from the ground and forest thicknesses (i.e. width perpendicular to shoreline). The results were measured in $H_{ct} = hc/ht$, where H_{ct} is a non-dimensional parameter, hc is crown height from the ground, and ht is tree height. Three H_{ct} numbers were generated: highest $H_{ct} = 0.7$, medium $H_{ct} = 0.5$, and lowest $H_{ct} = 0.3$.

The experiments indicated that flow structures are strongly influenced by the lowest crown height ($H_{ct} = 0.3$) and produce the most reduction in flow energy (40 – 43%). However, this produced scouring around the forest due to the high impact force of the overflowing water, which can significantly damage the forest. Optimum results that balanced energy reduction of the approaching current with minimum scouring were seen in the medium crown height ($H_{ct} = 0.5$) and the largest

possible forest thickness (i.e. width). It seems recommended that coastal forests be designed with a medium crown height considered and a maximized width (i.e. perpendicular to shoreline).

Tree Distribution

Tree breakage was analyzed in detail by Tanaka et al. (2018) to demonstrate the effectiveness of broken trees on tsunami flow energy reduction. Previous field surveys, physical experiments, and numerical simulations indicated the effectiveness of vegetation for decreasing tsunami run-up heights (Irtem et al. 2009; Ismail et al. 2012) and the reflection and transmission of a solitary wave (Huang et al. 2011), but most of these experiments were conducted using only a simplified tree model (i.e. circular cylinders) as the physical model of a coastal forest. Although previous studies indicated the importance of crown height (Sato et al. 2012) and two important breaking modes (Tanaka et al. 2013; 2015), not many studies focused on the crown structure of real trees. One study (Tanaka and Ogino 2017) directly compared the reduction of fluid force to the production of driftwood and secondary damage of coastal forests and concluded that the advantages of coastal forests outweighed the disadvantages.

The four objectives of this study were to: 1) analyze tree-breakage in detail considering the stand structure of trees (i.e. tree height, crown height, projected area of crown and trunk, and drag characteristics of leaves), 2) establish a coastal forest structure that produces less driftwood and also traps any driftwood that is produced, 3) reduce flow energy even when trees in a forest are partly or largely broken, and 4) determine important parameters for increasing the mitigation function of a coastal forest as a bioshield. A numerical simulation of two tsunami magnitudes to model drag force and destruction mode (i.e. breakage of tree trunk or tree overturning) was used to pursue these objectives.

The results indicated that the critical overturning moment for a tree is greatly affected by substrate conditions, number of roots, and root anchoring strength. Overturning was the dominant mode of actual destruction (81%) (Sato et al. 2012; Noguchi et al. 2012). When trunk breakage occurs, the upper part of a tree is washed out and driftwood is produced. Only the remaining trunk can provide

resistance to a tsunami, but at greatly reduced effectiveness. In the case of overturning, the fallen tree continues to provide drag even though the resistance is decreased, and the remaining part can help trap small debris. Due to erosion of the substrate, some trees may become driftwood even in overturning. During the 2011 GEJT, it was seen that production of whole tree driftwood was limited to scoured areas behind armaments or steps (Tanaka et al. 2013).

The study recommends a combination of two tree species or types in coastal forest design: a tree with a large resistance and a low crown on the seaward side and a tree with a high crown and a large diameter on the landward side. Larch and oak were mentioned, respectively. Larch trees can provide greater drag during the early stage of a tsunami as well as after breakage since the primary destruction mode is overturning. Oak trees tend to produce driftwood in most cases, but also withstand high tsunami water depth and trap driftwood when the tree trunk diameter exceeds a critical value. For trapping driftwood and remaining unbroken, a large trunk diameter is required. Trees for trapping debris should be located on the inland side of the forest or be a second forest inland, similar to the double-layered models in Tariq et al. (2021). By increasing crown height or trunk diameter, the second inland forest becomes a stronger shield for trapping driftwood and debris. To create a dense forest, tree crown shape should be slender.

Landform

Lunghino et al. (2020) analyzed the effect of hill structures on an incoming tsunami. Interactions between a single row of hills and an incoming tsunami were numerically modeled to test variables such as hill spacing, hill height, and hill shape. The findings indicate that a single row of hills can partially reflect the energy of an incoming wave and reduce the onshore kinetic energy. Tightly spaced hills were found to reflect more wave energy while smaller hills reflected less. In the event a tsunami wave height exceeds that of the hill height, the protective benefits of any hill structure are limited. The protective benefit of hills at a coastline is comparable to that of a small wall, and combining a wall and hills would duplicate the protective benefit and may not provide any clear added value. Hills could elevate the damage risk by increasing the flow speeds on the backside of the hill. To counter this, a buffer zone of smaller, staggered hills behind the first row of hills can

reduce the flow speeds of water before reaching populated areas further inland.

Performance Factors

Based on the literature review, five coastal forest composition elements have been identified as the greatest contributors to mitigation effects. They include aspect ratio, layering, crown height, distribution, and landform. Based on their scientific implications, these elements have been translated into factors that should guide the overall design of the forest in order to maximize tsunami mitigation impacts. Called Performance Factors, they include forest area, gap layering, tree crown height, tree distribution, and landform.

Forest Area

The overall shape of the forest affects how water flows around it. Ideally, the area of the forest should fall within a range of acceptable aspect ratios. Aspect ratio is the ratio of the forest's length (i.e. parallel to the coastline) to its width (i.e. perpendicular to the coastline). Ratios of less than 4 create turbulence on the inland side of the forest more so than if the forest did not exist, and ratios of greater than 4 reduce this turbulence. To avoid increased turbulence on the backend of the forest, the overall forest area should be an aspect ratio of 4 or greater (see fig. 28).



Figure 28. Diagram showing aspect ratio as a relationship between forest length and width. An aspect ratio of ≥ 4 is ideal. Image by Brook Goodwin (2022). Basemap image from Google Earth.

Gap Layering

Any gaps within the forest, such as a roadway or building, can create high flow velocities as water is channeled around the forest and through the gap. In cases where these gaps are necessary, alternating the placement of the gaps can counter the increased flow velocity. By layering the forest and alternating pathways through it, channelization and increased flow velocities can be avoided (see fig. 29).

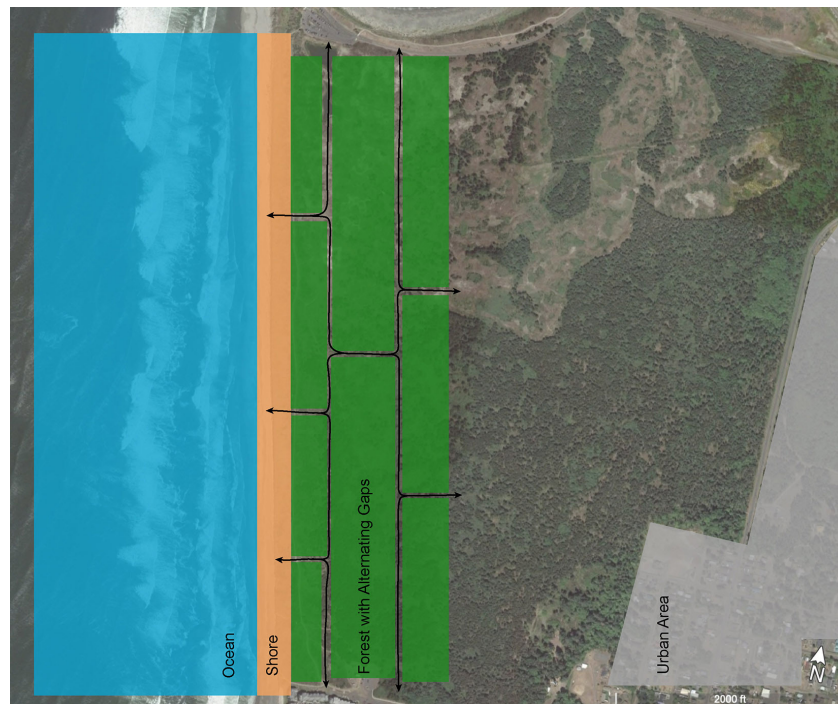


Figure 29. Diagram showing forest layout with alternating gaps. Alternating gaps can reduce channelization of flow. Image by Brook Goodwin (2022). Basemap image from Google Earth.

Tree Crown Height

When submerged and water is moving through them, the branches and leaves of trees, called crowns, create drag forces that slow the flow of water. The crown height, or the distance of the lower part of the crown from the ground, has varying effects on the flow structure of water moving through it. These heights can be categorized as low, medium, and high crown heights. A low crown height has the most influence on the flow, but produces excess soil erosion and scouring at the base of the tree. A medium crown height provides adequate drag force and flow reduction with minimal scouring. Choosing trees which have a medium crown height can maintain drag forces to slow the

flow of water while minimizing soil erosion (see fig. 30).

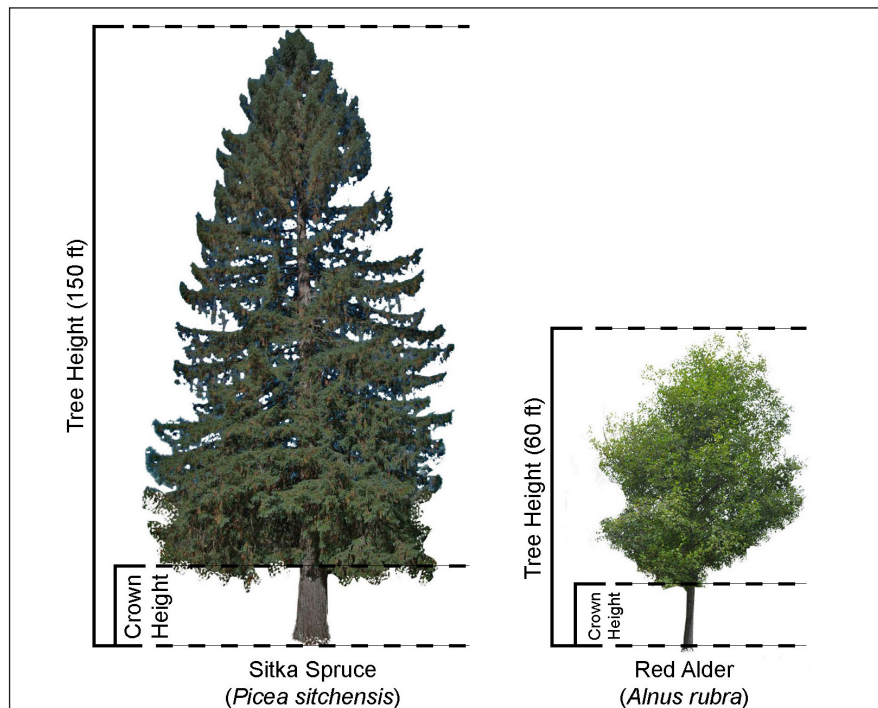


Figure 30. Diagram showing the relationship of overall tree height to crown height. Medium crown heights will provide drag force while reducing scouring. Image by Brook Goodwin (2022).

Tree Distribution

Tree distribution refers to the groupings of tree species between the seaward-facing area and the landward-facing area of the forest. The seaward-facing area should prioritize maximizing wave force resistance and drag force, while the landward-facing area should prioritize trapping driftwood and other debris and withstanding high tsunami waters (see fig. 31).



Figure 31. Diagram showing seaward species and landward species placement. Image by Brook Goodwin (2022). Basemap image from Google Earth.

In the seaward-facing area, wave force resistance will allow the trees to withstand the initial pushing forces of the incoming waves during the early stages of a tsunami, and drag force will help to slow down the flow of water through the trees. Trees with a low crown and a strong rooting habit are more ideal for this. The low crown will create drag as water moves through it and the strong roots will help keep the tree attached to the ground, even when overturned. Overturned trees will continue to create drag force as long as they remain anchored in place. Trees that break at the trunk or are pulled out of the ground get swept away and become driftwood.

In the landward-facing area, trapping driftwood and debris before it is swept further inland will reduce the amount of debris that reaches buildings and populated areas. Debris colliding with buildings and other objects is one of the primary forms of damage during a tsunami (Tanaka and Onai 2017). Trees with a large trunk diameter and high crown height are best suited for trapping debris and resisting breakage.

Landform

Hill structures provide resistances to tsunamis, primarily in the form of reflection of wave energy. A single row of hills near the shoreline, such as an established sand dune, can partially reflect the incoming wave energy and reduce the onshore kinetic energy. This protective benefit is comparable to that of a sea wall. However, combining a sea wall with hills would be redundant and not provide increased protection. Using one or the other is recommended, but not both. A single row of hills could unintentionally increase the flow speeds on the backside of the hill. To counter this effect, a buffer zone of a series of smaller hills behind the first row of hills is recommended. This buffer zone can reduce the flow speeds of the water before it reaches buildings and populated areas (see fig. 32).

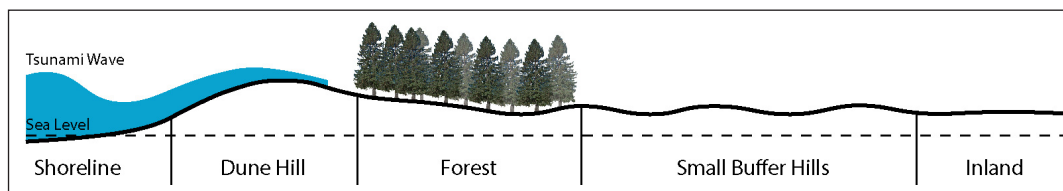


Figure 32. Diagram showing forest layout with alternating gaps. Alternating gaps can reduce channelization of flow. Image by Brook Goodwin (2022).

Effects of Factors

The Performance Factors can be summarized in terms of their desired effects on tsunami forces. Reflection of wave energy is achieved through hills and the seaward-facing tree species. Reduced flow speeds are through hills, dense crowns of seaward-facing tree species, debris trapping and strong trunks of landward-facing tree species, and alternating gaps. Reduced erosion is from medium tree crown heights and dense root structures. Reduced inundation depth is via hill height, but only for small and medium tsunamis that do not exceed the hill height.

Case Studies

Coastal Forest Restoration – Natori, Japan

Shortly after the 2011 GEJT, the Japanese government partnered with the Organization for Industrial, Spiritual, and Cultural Advancement (OISCA International) to restore a coastal forest in Natori, Japan. The forest was completely destroyed during the tsunami and held significant cultural and spiritual meaning to the local residents (see fig. 33 and 34). OISCA International, in an effort focused on community needs and economic relief, paid local farmers to help replant the forest. Since 2011, OISCA International has employed more than 8,000 tsunami survivors to plant over 370,000 Japanese black pine trees. Seedlings are grown in a nursery for the first two years and then transplanted (see fig. 35). This resulted in a 99% survival rate for the trees for seven consecutive years. The goal is to restore 100 hectares and the project is expected to continue until at least 2040 as the trees mature (see fig. 36) (Adler 2021).

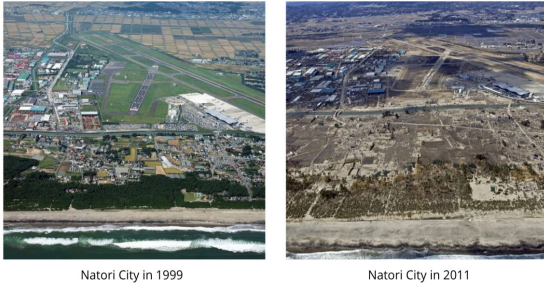


Figure 33. A before and after image of Natori City and its forest. Photo via OISCA International (*10 Years After The Tohoku Earthquake And Tsunami, Survivors Restore A Coastal Forest* n.d.).



Figure 34. A ground-level photo of the toppled forest. Photo via OISCA International (*10 Years After The Tohoku Earthquake And Tsunami, Survivors Restore A Coastal Forest* n.d.).



Figure 35. Japanese black pine seedlings are grown in a nursery for the first two years and then transplanted. Photo via OISCA International (*10 Years After The Tohoku Earthquake And Tsunami, Survivors Restore A Coastal Forest* n.d.).



Figure 36. Aerial photo of the forest restoration area. Photo via OISCA International (*10 Years After The Tohoku Earthquake And Tsunami, Survivors Restore A Coastal Forest* n.d.).

Tsunami Mitigation Parks – Japan, Indonesia, Chile

As part of the previously mentioned landform study, Lunghino et al. (2020) reviewed three recently and soon-to-be constructed tsunami mitigation parks in Japan, Indonesia, and Chile. These parks use a hybrid mitigation approach that combines vegetation with an engineered element. The authors make a distinction between hybrid parks like these and purely natural measures such as mangroves because they offer the possibility of strategic design. In their evaluations, the authors determined that most tsunami mitigation parks that are being built are informed more by design aesthetics than mitigation science. They intended the study to be a starting point for understanding how to design these parks to maximize their mitigation benefits. Below are the three projects mentioned in the study.

The park in Japan, called the Morino Project, is located in Tohoku. Tohoku was one of many areas affected by the 2011 GEJT. The project intends to build a 16-foot high embankment from soil and debris from the earthquake. Behind the embankment, a coastal forest of evergreen broadleaf trees will be planted (see fig. 37). The project is a way for residents to both build a forest and spiritually recover from the disaster by participating in community planting parties (see fig. 38 – 40) (“Morino Project” 2016).



Figure 37. A rendering that shows a hybrid mitigation park layout with a coastal forest and sea wall. Image by PUR Project (*Morino Project* 2016).



Figure 38. A recently planted section of forest in the Morino Project. Photo by Christian Lamontagne/PUR Project (Lamontagne 2016).



Figure 39. Forest restoration work being performed by community volunteers in the Morino Project. Photo by Christian Lamontagne/PUR Projet (Lamontagne 2016).



Figure 40. A section of recently planted seedlings in the Morino Project. Photo by Christian Lamontagne/PUR Projet (Lamontagne 2016).

In Indonesia, the National Mangrove Program intends to restore over 600,000 hectares of degraded mangroves by 2024 and improve conservation efforts of existing mangroves. This program is a partnership between multiple government ministries, civil organizations, and private sector organizations. This project also employs a landscape approach to mangrove management, restoring mangroves through planting and also ensuring sustainable management of existing mangroves through community incentives, regulations, and spatial planning (see fig. 41) (Kahkonen and Rodrigues de Aquino 2021).



Figure 41. The President of Indonesia, Joko Widodo (second from left), visiting mangrove replanting efforts in Tarakan by the National Mangrove Program. Photo by Bureau of Press, Media, and Information Affairs of Presidential Secretariat via World Bank Group (*Indonesia's 'Green Belt' – Mangroves for Local and Global Benefits 2021*).

In Chile, a reconstruction plan of Constitución was carried out by a team of architects in 2010 shortly after the country was struck by an 8.8 magnitude earthquake and tsunami. Through a participatory design process, residents were asked about what they wanted for the city. A historic lack of public space and democratic access to the river was a common complaint and request.

The project team devised a threefold strategy: 1) an alert and evacuation plan, 2) a coastal forest designed to maximize drag force and reduce a tsunami's wave energy, and 3) a conditioned building zone with collapsible enclosures in the lower levels (see fig. 42 and 43) (Busta 2016).



Figure 42. Aerial photo showing the shoreline of Constitución, Chile. Photo by Felipe Diaz via Architect Magazine (Diaz n.d.).



Figure 43. A before and after rendering of one of the forested park areas in Constitución, Chile. Image by Elemental via Architect Magazine (*Post-Tsunami Sustainable Reconstruction Plan of Constitución* 2010).

Application to the Pacific Northwest




Suitability Criteria

Populated areas along the Washington Pacific coast near Grays Harbor (see fig. 44) were evaluated for their suitability to host a tsunami-mitigating coastal forest. Within a 10-mile radius, seven populated areas were identified. These include smaller towns such as Ocean City, Oyehut-Hogans Corner, Cohasset Beach, Grayland, and North Cove, and two larger cities: Ocean Shores and Westport. Ocean Shores and Westport, as the only two coastal cities within the search area, were selected for further evaluation in criteria including Population, Inundation Depth Risk, Evacuation Times, Existing Measures, and Suitable Area Available. These criteria were formed into a matrix in order to compare the two cities and select one as a coastal forest study area (see table 1).



Figure 44. Context map showing location of Grays Harbor in Washington. Map by Brook Goodwin (2022). Basemap image from Google Earth. Data from Washington State Geospatial Portal.

Table 1. Matrix showing populated areas within 10-mile radius and a comparison of Ocean Shores and Westport. Maps by Brook Goodwin (2022). Basemap images from Google Earth. Data from US Census 2020, Eungard et al. (2018a), and *Westport Tsunami Evacuation Walk Times* (2019).

	<ul style="list-style-type: none"> • Populated areas along the Pacific coast near Grays Harbor were evaluated for their suitability to host a coastal forest • Ocean Shores and Westport are the largest cities in the coastal area 	
	<p>Ocean Shores</p> 	<p>Westport</p> 
Inundation Risk	20-60ft in most of city < 20ft inland-facing side (east of Duck Lake)	20-60ft in ocean-facing half < 20ft in inland-facing half and main city
Evacuation Times Routes	Very poor No high ground	0-15 min for most of city 15+ min along coast 30+ min in Half Moon Bay Multiple spots of high ground 50ft
Population (2020 Census)	6, 715	2, 213
Existing Measures	Sirens	Ocosta School evacuation tower Sirens Dunes High ground Beach armament
Suitable Area Available	Unavailable, highly subdivided and developed	Westport Light State Park

Based on the 2020 US Census, Ocean Shores has a population of 6,715 and Westport of 2,213. Both cities have high inundation depth risks of 20 – 60 feet in most areas according to current NOAA models and the Washington Geological Survey Map Series (Eungard et al. 2018a). In Ocean Shores, the evacuation times are very poor as the city has no adequate high ground nearby that can be reached, it is criss-crossed by canals with bridges vulnerable to collapse in an earthquake, and the only existing mitigation measures are sirens. In Westport, high ground exists as small hills of greater than 50 feet in elevation near the middle part of the city and larger hills of similar elevation further south near Cohasset Beach, connected by dune ridges that predate previous CSZ earthquakes and tsunamis (Peterson et al. 2010). Also near Cohasset Beach is the evacuation tower at Ocosta Schools. Given the proximity to high ground and based on information from the Washington State Department of Natural Resources (WA DNR) and NOAA (“Geologic Hazard Maps” n.d.), evacuation times are 0 – 15 minutes for most parts of the city, greater than 15 minutes along the ocean coast, and greater than 30 minutes in Half Moon Bay and the jetty. Existing mitigation measures include sirens, beach armament, the Ocosta School evacuation tower, and a well-established sand dune along the length of the coast.

Westport Tsunami Risk

Tsunami inundation risk in Westport is based on a WA DNR and NOAA Center for Tsunami Research tsunami hazard study and map series, produced in March 2018 (Eungard et al. 2018a). The study is based on tsunami model results from a ~2,500-year CSZ earthquake scenario (see fig. 46 and 47). In Westport, a tsunami will reach the ocean shore first and begin to flow inland on the city's western edge. Afterwards, it will make its way into Grays Harbor and then begin flowing inland from the other eastern side. The model indicates water current speeds of up to 9 knots or more as the tsunami makes its way inland from the ocean coast. It loses some speed as it makes its way into Grays Harbor to about 3 – 6 knots as it flows inland from the eastern side. Inundation depth levels vary between 10 – 15 feet in the more urban area on the eastern side and upwards of 30 – 60 feet on the western seaward-facing side. Tall hills that exceed elevations of 50 feet are the only high ground areas that remain dry. These hills are mainly in the southeastern edge of Westport Light State Park and south of the city near Cohasset Beach.

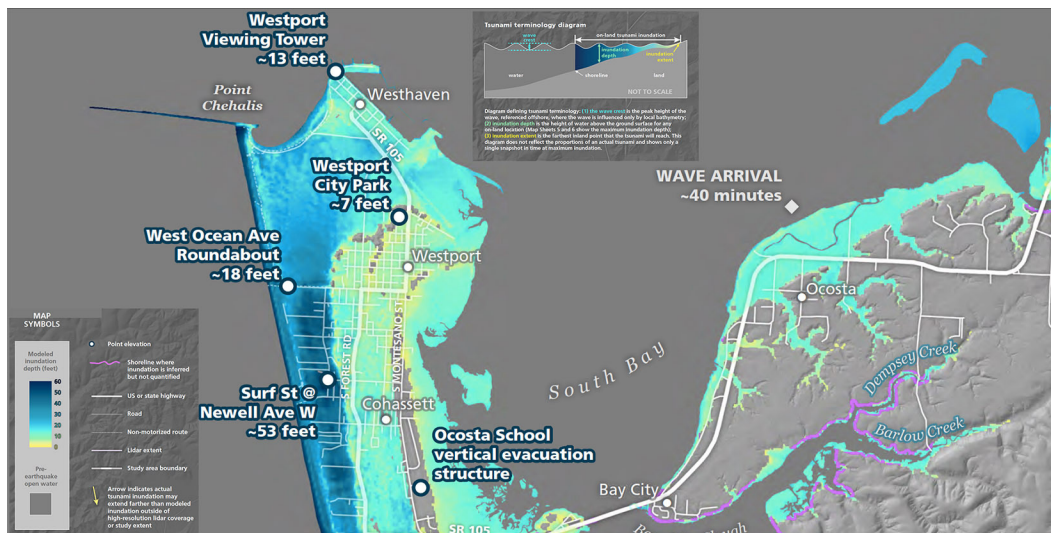


Figure 46. Map showing tsunami inundation depths for Westport, WA. Map by WA DNR/NOAA, cropped by Brook Goodwin (Eungard et al. 2018b).

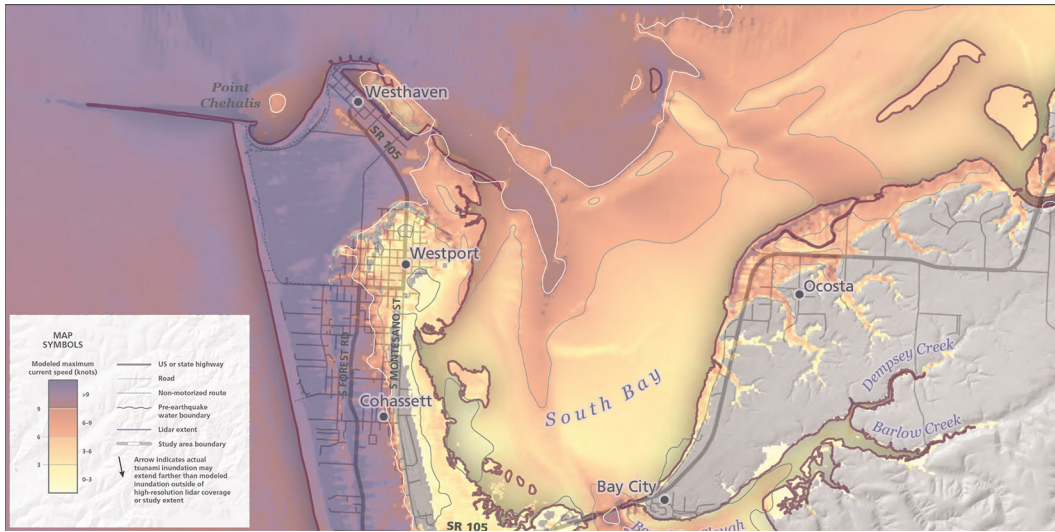


Figure 47. Map showing tsunami inundation speeds for Westport, WA. Map by WA DNR/NOAA, cropped by Brook Goodwin (Eungard et al. 2018c).

Based on the same NOAA tsunami model, the WA DNR also developed maps of evacuation route walk times for various cities including Westport (see fig. 48) (“Geologic Hazard Maps” n.d.). The map for Westport shows the estimated wave arrival times and the amount of time it would take to evacuate to safe high ground from different regions of the area. Most of the urban area of the city falls within the 0 – 15 minute zone, including the southern portion of the park. Most of the ocean coastline and the middle section of the park fall within the 15 – 30 minute zone. The northwest corner including Half Moon Bay falls within the 30 – 45 minute zone, and the jetty within zones of 45 – 50 minutes and greater. The estimated wave arrival time for the ocean coastline is as little as 15 minutes. The arrival time increases as the wave makes its way into Grays Harbor and loses flow speed. The arrival times are 25 minutes at the northern end of the marina, 35 minutes at the southern end of the marina, and 50 minutes at South Bay. Based on the arrival time of the wave at the ocean shoreline, the ideal evacuation time for any area of the city would be 15 minutes or less.

Existing Measures

Existing tsunami mitigation measures in Westport include warning sirens, beach armaments, and an evacuation tower, as well as an established dune and existing high ground. Four warning sirens are placed throughout the area at Ocosta School, the south side of the city near Newell Ave W, the middle of the city at Pacific Ave E and Montesano St, and near the marina at Bay St and Montesano St (indicated in fig. 48). Beach armaments in the form of 10 – 15 feet high rock walls are along the entire northern edge of the marina and around to Half Moon Bay (see fig. 49). Similar rock walls are along the jetty. One evacuation tower is located at Ocosta School just south of the city.



Figure 49. Rock wall beach armaments along the northern coast of Westport. Photo by Brook Goodwin (2022).

Site Analysis

The site for this design investigation is located within Westport Light State Park, a 560-acre day-use park with 1,215 feet of shoreline along the Pacific Ocean on its western edge and Half Moon Bay on its northern edge (see fig. 50 – 52). This park is part of the Washington State Park system and is the result of a consolidation of Westhaven and Westport Light state parks into one park in 2016. The

park is named after the historic Westport Lighthouse, also called Grays Harbor Lighthouse, built in 1898 and adjacent to the park on Coast Guard property. A paved 1.3 mile path runs along a dune on the edge of the shoreline (see fig. 53). A parking lot and restroom area is located at each end of this path on the south and north sides of the park (see fig. 54) (“Westport Light State Park” n.d.).



Figure 50. Context map showing the location of Westport Light State Park. Map by Brook Goodwin (2022). Basemap image from Google Earth.



Figure 51. Pacific shoreline of Westport Light State Park. Photo by Brook Goodwin (2022).



Figure 52. Half Moon Bay on the northern edge of Westport Light State Park. Photo by Brook Goodwin (2022).



Figure 53. Walking path along the dune in Westport Light State Park. Photo by Brook Goodwin (2022).



Figure 54. Restroom building at the northwestern corner of Westport Light State Park. Photo by Brook Goodwin (2022).

Ecologically, the park can be divided into four primary zones: shoreline, dune, shrubland, and forest (see fig. 55). The shoreline is from the ocean's edge to the dune and is mostly sand with some grass along the dune edge (see fig. 56). The dune is a well established sand dune with a mix of grasses and shrubs. Dunes can be split into three zones: foredune, dune plain, and backdune. The foredune is the shore-facing slope and is typically mostly grasses (also seen in fig. 56). The dune plain is the top part of the dune and is flatter with a mix of shrubs and grasses (see fig. 57). The backdune is the inland-facing slope and is mostly shrubs with some grasses (see fig. 58). The shrubland is a low-lying area in the middle area of the park with moderately wet soil and groupings of shrubs and small coniferous trees (see fig. 59). The forest comprises the eastern half of the park and is of mostly coniferous, medium-height trees (see fig. 59 and 60).



Figure 55. Map showing the areas of shoreline, dune, shrubland, and forest. Map by Brook Goodwin (2022). Basemap image from Google Earth.



Figure 56. Ocean shoreline and foredune. Photo by Brook Goodwin (2022).



Figure 57. Dune plain and walking path. Photo by Brook Goodwin (2022).



Figure 58. Backdune and shrubs. Photo by Brook Goodwin (2022).



Figure 59. Shrubland (foreground) and forest (background). Photo by Brook Goodwin (2022).



Figure 60. Forest area near the lighthouse. Photo by Brook Goodwin (2022).

The site for this design investigation is a rectangular area that runs parallel to the coastline along the edge of the dune and shrubland (see fig. 61). The site is roughly 5,000 feet long and 1,250 feet wide. This is the maximum length of unobstructed area, situated in shrublands between the northern and southern parking lots. A width of 1,250 feet maintains a 4:1 aspect ratio, as recommended in the forest area Performance Factor.



Figure 61. Map showing the study area within the park. Map by Brook Goodwin (2022). Basemap image from Google Earth.

Soils

The following soil composition information for Westport is based on a United States Department of Agriculture (USDA) Natural Resources Conservation Service soil survey report from 1986. In summary, the soil was formed from dune sand and is mostly fine sand with a thin layer of grass, moss, leaves, and needles. Water permeability is high and the available water capacity is low. Effective rooting depth is generally about 5 feet or more, but may be restricted by lack of moisture or nutrients. The risk of water erosion is low but the risk of soil blowing from wind is severe. It is recommended that disturbed areas be re-vegetated as soon as possible to control soil blowing (Pringle 1986).

153-Westport fine sand, 3 to 10 percent slopes.

This very deep, excessively drained soil is on long, narrow, stabilized sand dunes. It formed in slightly weathered dune sand. The native vegetation is mainly grass and shore pine. Elevation is 10 to 50 feet. The average annual precipitation is 60 to 80 inches, the average annual air temperature is about 50 degrees F, and the average growing season (at 28 degrees) is 200 to 240 days.

Typically, the surface is covered with a thin mat of grass, moss, leaves, and needles. The surface layer is very dark grayish brown fine sand about 7 inches thick. The upper 9 inches of the underlying material is dark grayish brown fine sand, and the lower part to a depth of 60 inches or more is olive gray fine sand.

Included in this unit are about 5 percent Yaquina soils and 1 percent Seastrand soils. Also included in some mapped areas are as much as 5 percent Netarts soils and 5 percent Dune land.

Permeability of this Westport soil is very rapid. Available water capacity is low. Effective rooting depth generally is 60 inches or more, but it may be restricted by a lack of moisture

and nutrients. Runoff is slow, and the hazard of water erosion is slight. The hazard of soil blowing is severe.

This unit is used as sites for homes and commercial buildings.

This unit is well suited to homesite development. If the density of housing is moderate to high, community sewage systems are needed to prevent contamination of water supplies as a result of seepage from onsite sewage disposal systems. Re-vegetating disturbed areas around construction sites as soon as possible helps to control soil blowing.

This map unit is in capability subclass VIe. (Pringle 1986, 108)

Topography

Topography elevation information is based on a LiDAR survey of 1-foot contours, provided by the Grays Harbor County GIS office (see fig. 62). The topography of the area around and including the site is mostly flat at about 15 feet elevation. Along the western edge is the existing dune and to the east is the existing shrubland and forest area. In the southeast corner are a series of high hills.

The shoreline slopes up gradually from sea level for about 200 feet to where the dune begins. The foredune slope is steeper and continues for about 100 – 200 feet before reaching the dune plain at around 30 feet elevation. The dune plain is the top of the dune and is mostly flat and about 100 – 200 feet wide. The backdune slopes downward from about 30 feet elevation to 15 feet elevation in a varying width of 100 – 300 feet. The shrubland and forest area is wide and very flat at about 15 feet elevation with variations up to 2 feet elevation. This area is about 1,000 – 1,500 feet wide in the southern area of the park and widens to upwards of 3,500 feet or more in the northern area. In the southeast edge of the park, the shrubland and forest area is met by steeply sloped hills that separate this area of the park from the urban edge of the city. These hills are about 45 – 50 feet elevation and considered safe high-ground for tsunami events. They vary in width from about 300 – 500 feet.

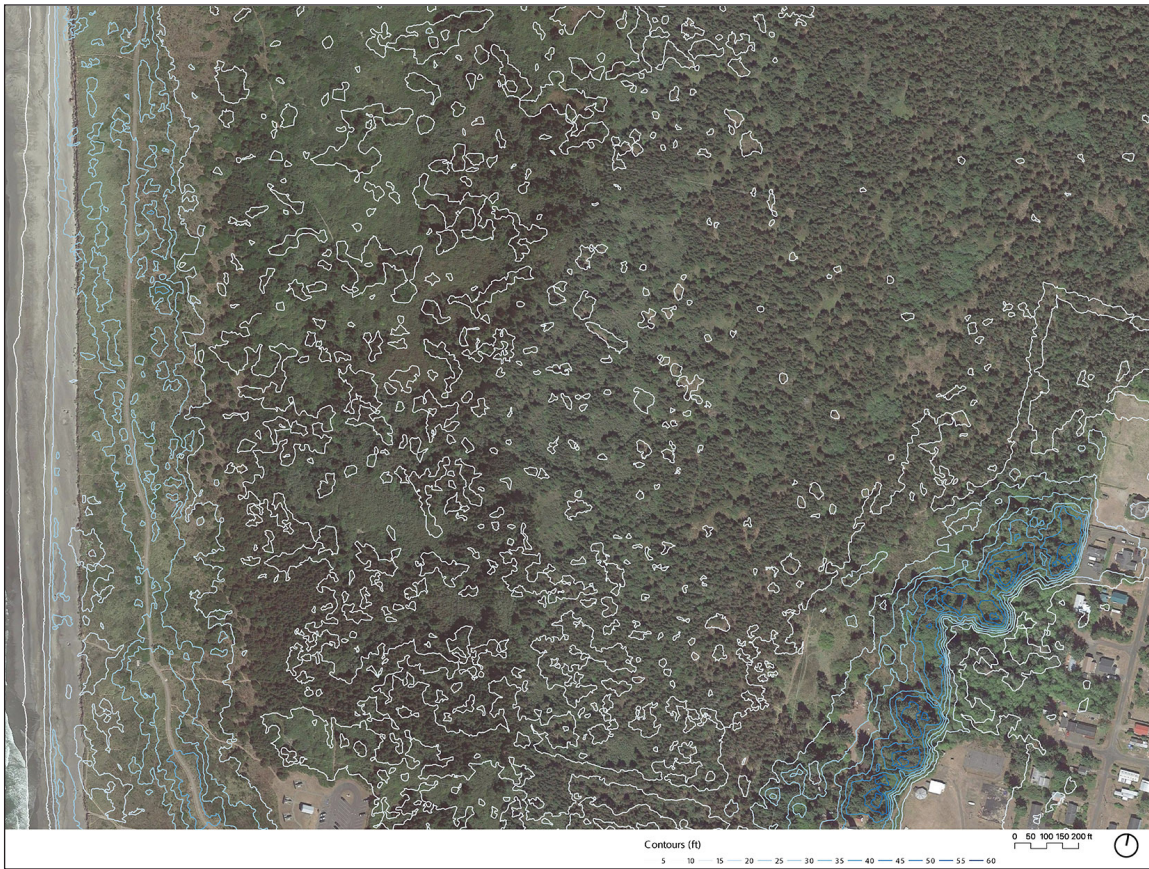


Figure 62. Color-coded 5-foot contour map, higher elevation contour lines are shown in blue. Map by Brook Goodwin (2022). Basemap image from Google Earth. Data from Grays Harbor County GIS.

Plant Inventory

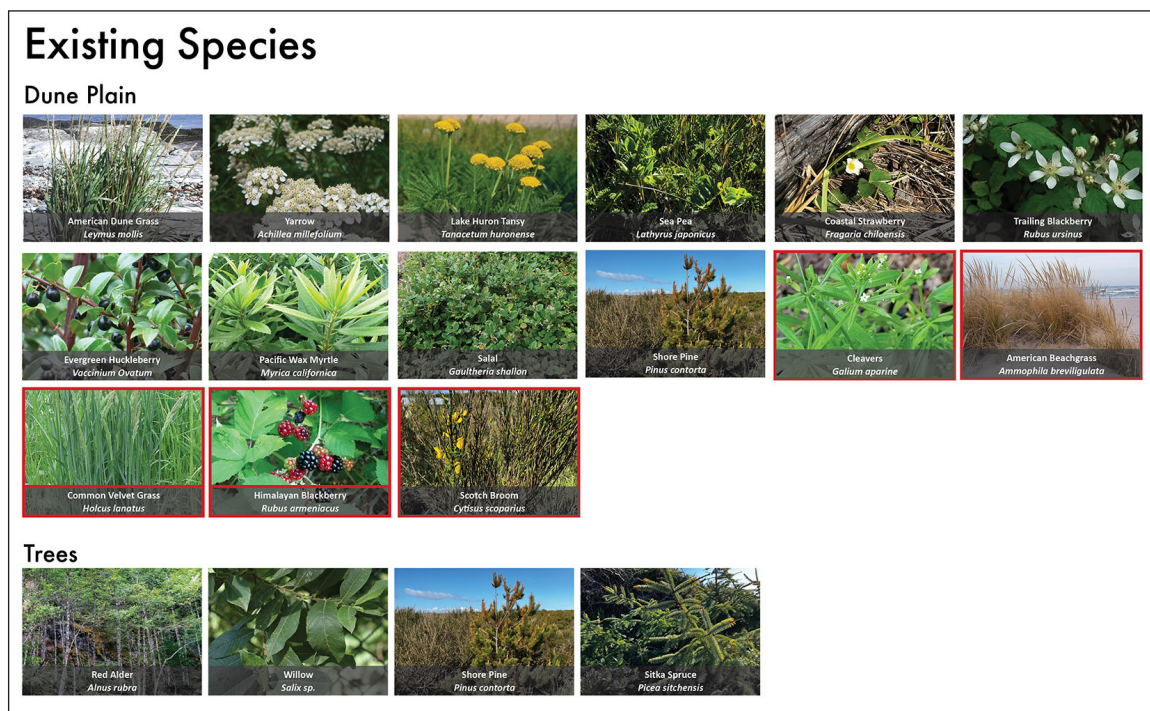
A site visit was conducted in April 2022 and a plant inventory of the dunes, shrublands, and forest was performed (see table 2 and 3). Overall, the dune was mostly a mix of native American dune grass and non-native American beach grass. Sea pea, another native, was also present and Scotch broom, an extremely invasive shrub, was very prominent throughout the entirety of the dune. The dune plain contained more native shrubs such as evergreen huckleberry, Pacific wax myrtle, salal, and trailing blackberry. Some native herbaceous plants including yarrow, Lake Huron tansy, sea pea, and coastal strawberry were also present. Small individual shore pines were spaced along the length of the dune plain. Multiple invasive species were also identified such as cleavers, common velvet grass, Himalayan blackberry, and Scotch broom. The backdune was lower and had wetter soil than either the dune plain or the foredune. The same shrubs from the dune plain were also present along with sword fern and rose spirea. Slough sedge was also found along with juniper haircap, a

small moss-like groundcover. Short shore pines and Sitka spruces were grouped throughout the backdune, becoming taller and denser as it transitioned into shrubland and then the forest. The forest area was mostly medium-sized shore pines with some Sitka spruce and red alder mixed in. An unidentified species of willow appeared in some areas near the edges of the forest.

Table 2. Planting palette showing existing foredune and backdune plant species. Invasive species are outlined in red. Image collage by Brook Goodwin (2022). Data from April 2022 field visit and plant inventory conducted by Brook Goodwin.



Table 3. Planting palette showing existing dune plain and forest plant species. Invasive species are outlined in red. Image collage by Brook Goodwin (2022). Data from April 2022 field visit and plant inventory conducted by Brook Goodwin.



Design Investigation

Tree Selection

According to the USDA, Westport and Grays Harbor fall within the Major Land Resource Area (MLRA) known as the Sitka Spruce Belt (see fig. 63). This zone is of forested areas that typically feature Sitka spruce as the dominant tree species. Its associated trees include shore pine, Douglas fir, western red cedar, western hemlock, big leaf maple, red alder, Pacific crabapple, red-osier dogwood, Oregon ash, black cottonwood, and multiple species of willow. Understory plantings consist mostly of shrubs and herbaceous plants such as Nootka rose, Pacific ninebark, red elderberry, salmonberry, Indian plum, snowberry, salal, and vine maple (“Trees and Shrubs for Riparian Plantings” 2010).

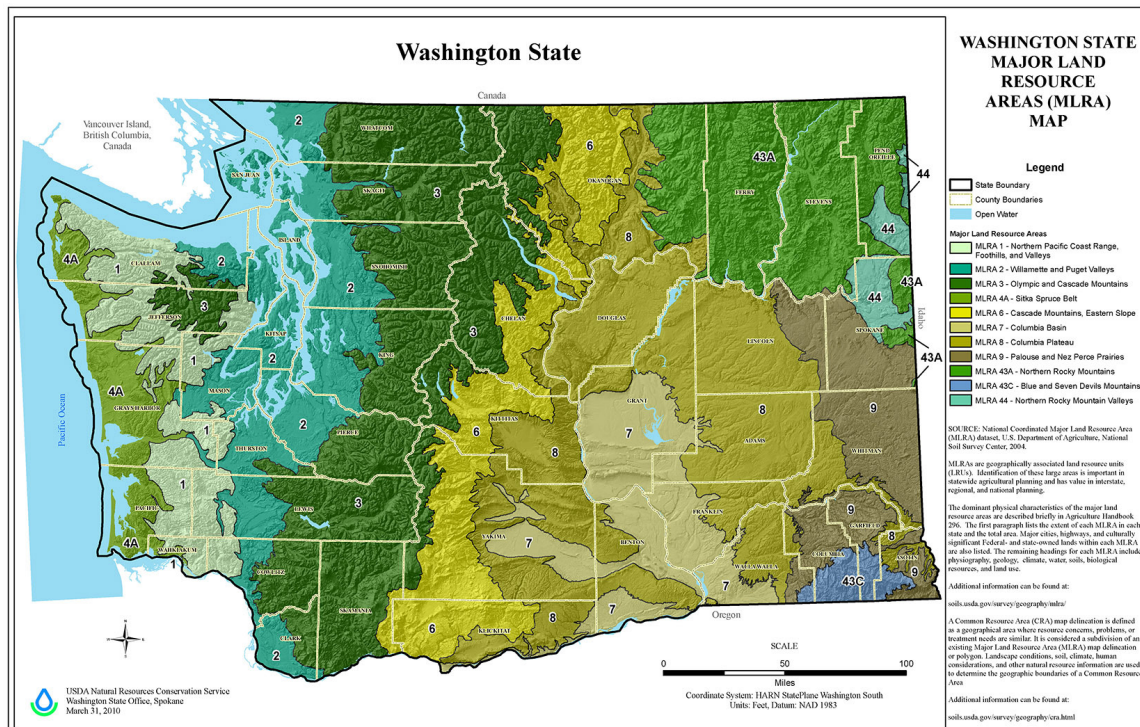


Figure 63. USDA MLRA map showing Sitka Spruce Belt in Grays Harbor, WA. Map by USDA Natural Resources Conservation Service (*Washington State Major Land Resource Areas (MLRA) Map* 2010).

When selecting the proposed tree species for the coastal forest, Sitka spruce was selected first along with four of its associated tree species: western red cedar, western hemlock, big leaf maple, and red alder (see fig. 64 and table 4). Western red cedar and western hemlock were chosen as complimentary coniferous trees to Sitka spruce and feature comparatively different growth rates, heights, and sizes. Big leaf maple and red alder were chosen as soil building deciduous trees that appear in multiple ecological zones. Associated understory plantings that would be well adapted to the well draining and sandy soil were chosen to complement these five tree species.

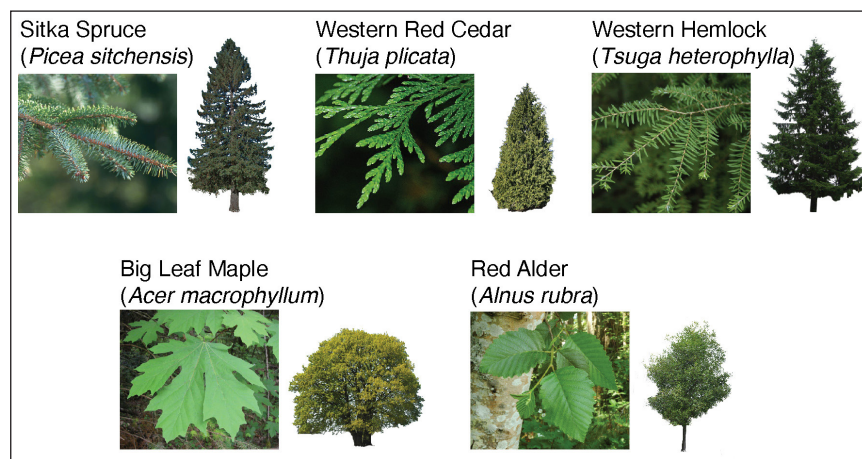


Figure 64. Image collage of the proposed trees. Collage by Brook Goodwin (2022).

Table 4. Proposed tree schedule with details for each of the five trees. Data from USDA (Harrington n.d.; Harris n.d.; Minore n.d.; Minore and Zasada n.d.; Packee n.d.).

Tree Schedule						
Common Name	Scientific Name	Growth Rate	Maturity	Height	Trunk Diameter	Crown Spread
Sitka Spruce	<i>Picea sitchensis</i>	4-5ft per year	30-40 years; 150ft	Avg: 150-200ft, Max: 250ft	4-6ft	30ft
Western Red Cedar	<i>Thuja plicata</i>	2-3ft per year	10-20 years; 70ft	Avg: 80-90ft, Max: 150ft	7-13ft	30ft
Western Hemlock	<i>Tsuga heterophylla</i>	1-2ft per year	25-30 years; 60ft	Avg: 165-200ft, Max 250ft	3-5ft	50ft
Big Leaf Maple	<i>Acer macrophyllum</i>	3-4ft per year	10-15 years; 50ft	Avg: 50ft, Max: 100ft	6-36in, avg 20in	40-70ft
Red Alder	<i>Alnus rubra</i>	2-4ft per year	15-20 years ; 60ft	Avg: 60-120ft, Max: 130ft	10-34in	20-30ft

Common Name	Rooting Habit	Category	Notes
Sitka Spruce	Long lateral roots; Rooting depth 6ft	Back, some mid and front	Intermediate shade tolerant
Western Red Cedar	Extensive roots	Back, some mid	Shade tolerant
Western Hemlock	Shallow roots; no taproot	Some front and mid	Shade tolerant
Big Leaf Maple	Shallow, widespreading root system;	Front, some mid and back	Soil builder
Red Alder	Extensive, fibrous root systems; ectomycorrhizal	Front, mid, back	Pioneer, Nitrogen fixer

Five Tree Species

Sitka spruce is the primary tree selected for this area given its dominant position within the Sitka Spruce Belt. These trees feature a wide trunk diameter of 4 – 6 feet, crown spread of 30 feet, and average height of 150 feet. They have long, lateral roots that can reach a depth of up to 6 feet (Harris n.d.).

Western red cedar is a prominent coniferous species in multiple ecological zones throughout western Washington, including the Sitka Spruce Belt. This tree features a wide trunk diameter of 7 – 13 feet, crown spread of 30 feet, and average height of 80 – 90 feet with an extensive rooting habit (Minore n.d.).

Western hemlock is another prominent coniferous species that shares associations with multiple native trees in western Washington. The trunk diameter is narrower at 3 – 5 feet, but the crown spread is wider at 50 feet and average height greater at 165 – 200 feet. The roots are shallow with no taproot (Packee n.d.).

Big leaf maple is a commonly found deciduous tree throughout western Washington and has some of the largest leaves of any maple species. The trunk size is narrower than that of the three conifers at 0.5 – 3 feet. It has a wider crown spread of 40 – 70 feet, an average height of 50 feet, and shallow wide-spreading roots. It is also a soil builder due to its large leaves forming dense leaf litter in the autumn and winter (Minore and Zasada n.d.).

Red alder is another common deciduous tree in western Washington. It has a narrow trunk diameter of 1 – 3 feet, a crown spread of 20 – 30 feet, and an average height of 60 – 120 feet. It is often one of the first tree species to grow in the early stages of forest regrowth and is regarded as an establishment tree. Its roots are fibrous, extensive, and ectomycorrhizal as a nitrogen fixer (Harrington n.d.).

Understory Plantings

Shrubs, herbaceous, and groundcover plants that are suitable for the soil type and commonly associated with the five tree species were chosen to comprise the understory of the forest, based on data from the USDA (Harrington n.d.; Harris n.d.; Minore n.d.; Minore and Zasada n.d.; Packee n.d.). Some native plants that currently exist in the shrubland area of the site were also included. The proposed plants are evergreen huckleberry, Pacific wax myrtle, salal, Pacific ninebark, salmonberry, vine maple, thimbleberry, Oregon grape, red huckleberry, oceanspray, Pacific rhododendron, sword fern, deer fern, Oregon oxalis, and evergreen violet (see table 5 and 6).

Table 5. Planting palette showing proposed understory plant species. Image collage by Brook Goodwin (2022). Data from USDA (Harrington n.d.; Harris n.d.; Minore n.d.; Minore and Zasada n.d.; Packee n.d.).



Table 6. Proposed understory plant schedule with details for each species. Data from USDA (Harrington n.d.; Harris n.d.; Minore n.d.; Minore and Zasada n.d.; Packee n.d.).

Understory Schedule				
Common Name	Scientific Name	Tree Associations	Category	Notes
Sword Fern	<i>Polystichum munitum</i>	Sitka Spruce, Western Hemlock, Big Leaf Maple, Red Alder	Fern	
Deer fern	<i>Struthiopteris spicant</i>	Western Red Cedar, Western Hemlock	Fern	
Evergreen Violet	<i>Viola sempervirens</i>	Sitka Spruce, Western Red Cedar, Western Hemlock	Herbaceous	
Oregon Oxalis	<i>Oxalis oregana</i>	Sitka Spruce, Western Red Cedar, Western Hemlock, Big Leaf Maple, Red Alder	Herbaceous	
Salal	<i>Gaultheria shallon</i>	Sitka Spruce, Western Red Cedar, Western Hemlock, Big Leaf Maple, Red Alder	Herbaceous	
Pacific Wax Myrtle	<i>Myrica californica</i>	Dune plain, Back Dune	Shrub	Nitrogen fixer
Red Huckleberry	<i>Vaccinium parvifolium</i>	Sitka Spruce, Western Red Cedar, Western Hemlock	Shrub	
Pacific Rhododendron	<i>Rhododendron macrophyllum</i>	Sitka Spruce, Western Red Cedar, Western Hemlock, Big Leaf Maple	Shrub	Out of range, but could exist
Evergreen Huckleberry	<i>Vaccinium ovatum</i>	Sitka Spruce, Western Red Cedar, Western Hemlock, Big Leaf Maple	Shrub	
Pacific Ninebark	<i>Physocarpus capitatus</i>	Western Hemlock	Shrub	Restoration, bank stabilization
Oceanspray	<i>Holodiscus discolor</i>	Western Hemlock	Shrub	
Vine Maple	<i>Acer circinatum</i>	Western Hemlock, Big Leaf Maple, Red Alder	Shrub	
Thimbleberry	<i>Rubus parviflorus</i>	Western Hemlock, Big Leaf Maple, Red alder	Shrub	
Salmonberry	<i>Rubus spectabilis</i>	Western Red Cedar, Western Hemlock, Big Leaf Maple, Red Alder	Shrub	
Oregon Grape	<i>Mahonia aquifolium</i>	Western Red Cedar, Western Hemlock, Big Leaf Maple, Red Alder	Shrub	

Tree Distribution

The forest area was divided into three sections: front, middle, and back. Based on the tree distribution Performance Factor, each of the five tree species was designated a location in either the front or back section of the forest area. The front section features trees with a lower and wider crown and a strong rooting habit. This maximizes drag force and keeps the trees anchored to the ground if overturned. The back section features trees with a wide trunk diameter and a higher and narrower crown. When positioned in dense stands, this allows the back section of trees to capture debris and driftwood. The middle section is a mixed transition of both the front and back sections. All five trees are included in each section, but their prominence and percentage may differ between sections. Trees in the front section are mostly western hemlock and big leaf maple, and trees in the back section are mostly Sitka spruce and western red cedar. As an establishment tree and nitrogen fixer, red alder is mixed evenly throughout both the front and back sections.

A diagram was created to show the distribution of the five tree species (see fig. 65). This diagram is not a planting plan nor does it indicate the exact placement for each tree; it merely represents the distribution of the tree species. Within each section, each of the five species was assigned a certain percentage and then randomly distributed throughout the section. Each section's percentage is as follows in the order of spruce, cedar, hemlock, maple, alder. Front: 17, 9, 20, 37, 17; Mid: 18, 18, 18, 28, 18; Back: 31, 31, 8, 15, 15. The bars at the bottom of the diagram also show this distribution.

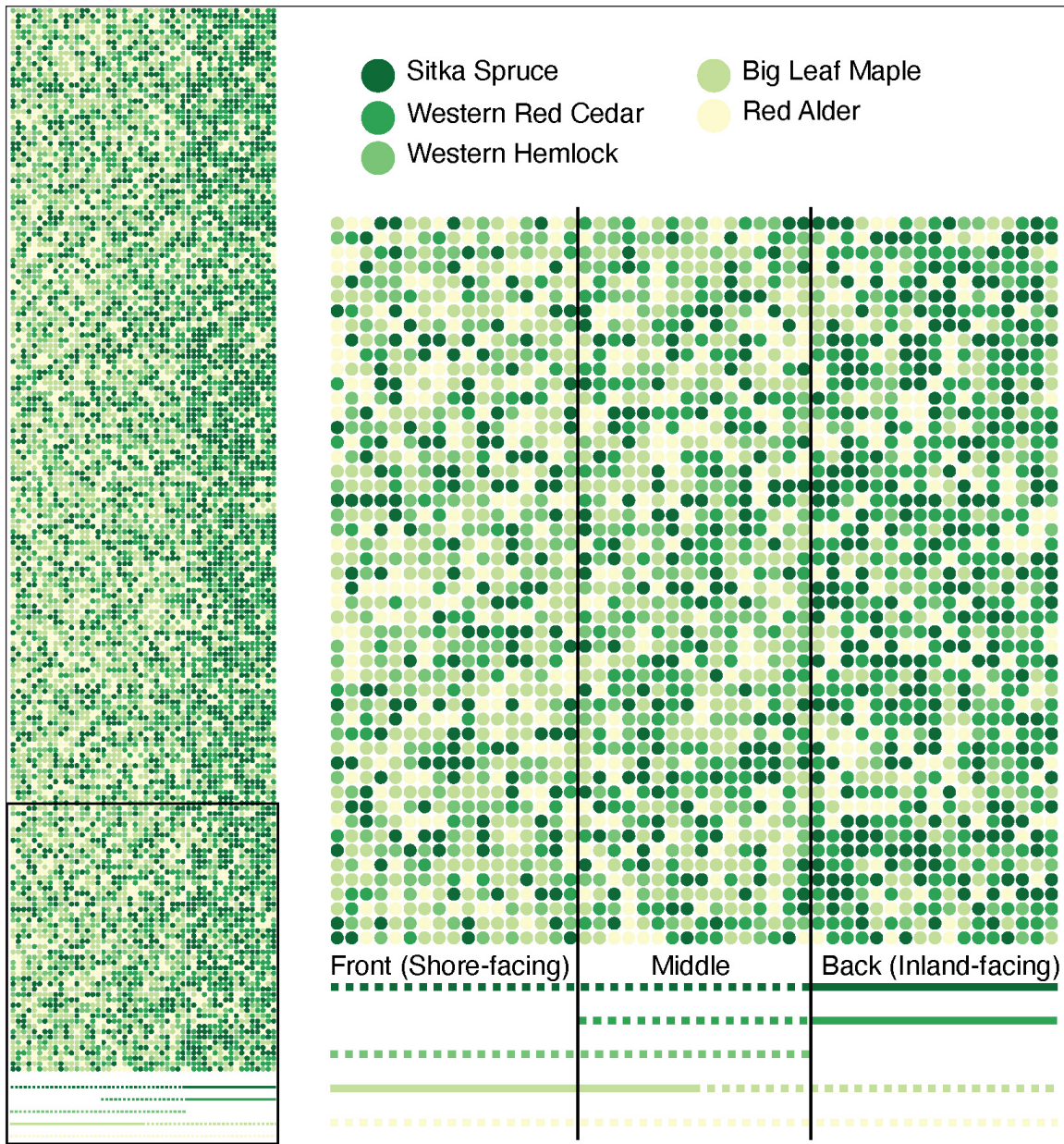


Figure 65. Diagram showing tree species distribution within the proposed forest area. Diagram is intended to be representational and not a planting plan with exact plant locations. Within each section, each of the five species was assigned a certain percentage and then randomly distributed throughout the section. Each section's percentage is as follows in the order of spruce, cedar, hemlock, maple, alder: Front: 17, 9, 20, 37, 17; Mid: 18, 18, 18, 28, 18; Back: 31, 31, 8, 15, 15. The bars at the bottom of the diagram also show this distribution. Image by Brook Goodwin (2022).

Landform

The existing dunes along the western edge and the hills along the southeast edge of the park are excellent landforms to work in combination with the coastal forest area (see fig. 66). The dunes are an average of 30 feet in elevation and can provide a strong buffer against small- to medium-sized tsunami waves, as suggested by Lunghino et al. (2020) and shown previously in fig. 32. The hills are about 40 – 50 feet in elevation and are considered safe high-ground during a tsunami event. After the landward-facing edge of the coastal forest, a buffer zone of a series of smaller, staggered hills should be created to reduce the flow speeds of water before reaching populated areas further inland.

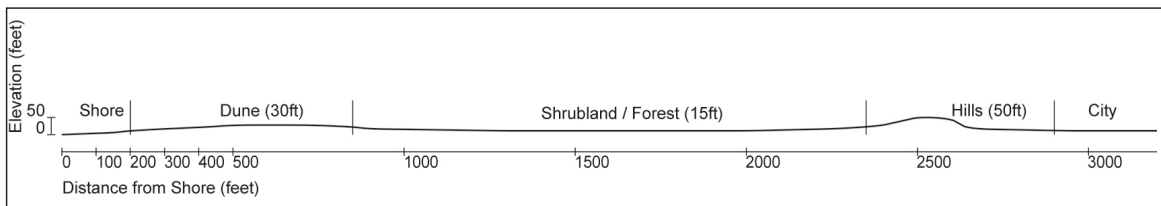


Figure 66. Section A (as indicated on fig 61) showing the topography of a southern section of the site, facing north. Distance is measured from the shoreline to inland. Image by Brook Goodwin (2022).

Phasing

Coastal forest development can be split into four phases: Phase 1 Establishment, Phase 2 Trails and Campgrounds, Phase 3 Interplanting, and Phase 4 Maintenance (see fig. 67).

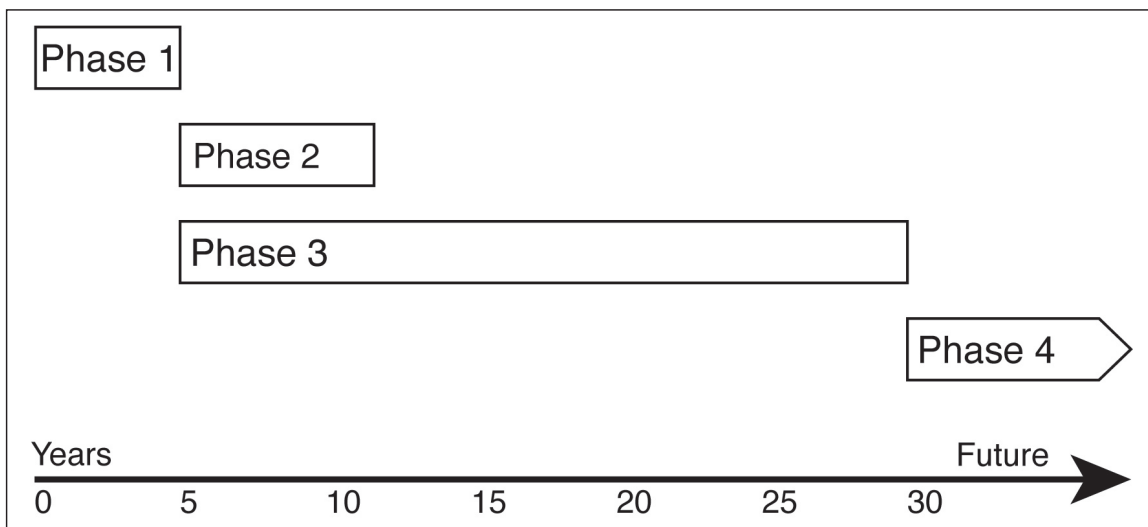


Figure 67. Phasing diagram showing how the phases relate to one another along a timeline. Image by Brook Goodwin (2022).

Phase 1 is the establishment phase of the forest. This phase focuses on the first five years of site development and includes clearing weeds, invasive species, and unwanted native plants. After clearing, any necessary changes to topography and soil amendments should be made before planting. Early plantings of hardy, sun-tolerant species should be made as well as tree saplings.

Phase 2 is about creating trails and campgrounds for recreation. This can start after the first plantings of trees are established and large enough to provide some shade, or within the first 5 – 10 years. A network of trails and campgrounds throughout the coastal forest will provide recreational opportunities that can be part of an ecotourism economic development program for the city.

Phase 3 is the interplanting phase. This phase occurs after early plantings from Phase 1 are established and continues until most of the trees reach maturity, or about 30 years. During this time, additional tree species and understory species can be planted, including those that require shaded areas.

Phase 4 is a continual maintenance phase that can last for 30 years or more. As the first plantings of trees establish and mature, they will require ongoing monitoring and maintenance by forestry specialists to ensure proper health and development. Trail and campground maintenance will need to be performed by Washington State Parks officials.

Discussion – Conclusion

Tsunami Mitigation Potential

Coastal forests have clear potential for tsunami mitigation. When designed with the five Performance Factors in mind (forest area, gap layering, tree crown height, tree distribution, landform), they can have direct effects on a tsunami's wave energy, flow speed, inundation depth, and inundation extent. A forest area aspect ratio of 4 or greater can reduce turbulent forces on the back end of the forest. Alternating and layering any gaps within the forest, such as roads, can reduce any flow channelization. Selecting trees with medium-sized crown heights can provide adequate drag force with minimal soil erosion and scouring. Distributing trees based on trunk diameter, crown height and shape, and rooting habit can help maximize drag force at the front of the forest and debris capture at the back. Combining the forest with an established dune or a sea wall can provide additional wave reflection and even hold back small- to medium-sized tsunamis. A series of buffer hills behind the dune can dampen the flow of any waves that exceed the height of the dune before they go further inland.

Changes to Tsunami Risk

Given the tsunami mitigating properties of a coastal forest, there is potential for changes to Westport's tsunami risk in terms of inundation rate. At its maximum drag potential, the forest could reduce the flow rate of a tsunami wave over land. This could increase the time it would take for the water to reach populated areas and give people more time to evacuate to safe high ground. Even as little as five extra minutes would be significant. The forest could also trap any debris and driftwood before it washes into areas with structures and buildings. This would reduce the amount of damage to structures from debris collision.

Influence on Future Site Developments

As previously mentioned, the Washington State Parks and Recreation Commission is considering a proposal by Westport Golf Links, Inc. for the development of a new Scottish links-style artisanal golf course, lodge, and facilities within the park. Their timeline projects completion of a proposed master plan and long-term lease agreement by June 2023. In its current state, the preliminary plan of the golf course (shown previously in fig. 45) intersects and abuts the study area chosen for the design investigation (shown previously in fig. 61). Based on the preliminary plan, the golf course's layout seems to place the fairway areas and the main parts of the course along the periphery of the park, leaving most of the shrublands and forest areas in the center as-is. The designers indicate this unused area as low-lying and wetland-like and wish to avoid developing it ("Jan. 26, 2022 Washington State Parks Regular Commission Work Session" 2022).

This undeveloped area has the potential to be designed as a coastal forest for tsunami mitigation. This design process could be carried out very similarly to the study area discussed in the Design Investigation section. The area could simply be scaled down to fit within the undeveloped area of the golf course (see fig. 68). As long as the forest aspect ratio stays at 4 or greater, all of the same design parameters and Performance Factors can be maintained. Gap layering can be used to accommodate any intersections of the forest with the paths that run through the golf course plan. If future site developments include new vertical evacuation structures, these paths can help connect areas of greater evacuation times, such as the Westport Jetty, Half Moon Bay, and the western shoreline, to new safe areas.



Figure 68. Map showing the potential area for coastal forest development within the proposed golf course plan. Map by Westport Golf Links, Inc (“Jan. 26, 2022 Washington State Parks Regular Commission Work Session” 2022). Modified with overlay by Brook Goodwin.

Further Research

Further research on the properties of coastal forests that can contribute to tsunami mitigation need to be carried out. Research in areas such as soils and geoen지니어ing could inform how changes in landform affect the flow of a tsunami wave. Forest restoration specialists could determine the best locations and tree and plant species to optimize the forest’s mitigation properties as part of a combined tsunami mitigation and habitat restoration initiative. Park and campground site designers can lay out trails and campsites in such a way as to minimize open gaps and reduce the chance of channelization. Economic development officials can work with the local city to develop recreational tourism programs that utilize the forest’s park and campgrounds to attract visitors. Opportunities for interpretive education about tsunamis, tsunami mitigation, and disaster preparedness may also be present.

References

- 10 Years After The Tohoku Earthquake And Tsunami, Survivors Restore A Coastal Forest*. n.d. Photo. OISCA International. Natori, Japan. Accessed May 18, 2022. <https://www.globalgiving.org/learn/10-years-tohoku-earthquake-and-tsunami/>. Archived at <https://web.archive.org/web/20210619065302/https://www.globalgiving.org/learn/10-years-tohoku-earthquake-and-tsunami/>.
- Adams, John. 1996. "Paleoseismology in Canada: A Dozen Years of Progress." *Journal of Geophysical Research: Solid Earth* 101 (B3): 6193–6207. <https://doi.org/10.1029/95JB01817>.
- Adler, Sam. 2021. "10 Years After The Tohoku Earthquake And Tsunami, Survivors Restore A Coastal Forest." GlobalGiving. March 16, 2021. <https://www.globalgiving.org/learn/10-years-tohoku-earthquake-and-tsunami/>.
- Ali, Arshad, and Norio Tanaka. 2020. "Experimental Study of Scouring Downstream of Coastal Vegetation in an Inundating Tsunami Current." *Landscape & Ecological Engineering* 16 (4): 273–87. <https://doi.org/10.1007/s11355-020-00420-z>.
- Anjum, Naveed, Norio Tanaka, and Md Abedur Rahman. 2021. "Role of Tree Crown Height for Effective Mitigation Capability of Inland Coastal Forest Considering the Flow Structures and Scour Phenomena." *Ocean Engineering* 238 (October): 109728. <https://doi.org/10.1016/j.oceaneng.2021.109728>.
- Atwater, Brian F. 1987. "Evidence for Great Holocene Earthquakes along the Outer Coast of Washington State." *Science* 236 (May): 942–45.
- . 1992. "Geologic Evidence for Earthquakes during the Past 2000 Years along the Copalis River, Southern Coastal Washington." *Journal of Geophysical Research: Solid Earth* 97 (B2): 1901–19. <https://doi.org/10.1029/91JB02346>.
- Atwater, Brian F., and Eileen Hemphill-Haley. 1997. *Recurrence Intervals for Great Earthquakes of the Past 3,500 Years at Northeastern Willapa Bay, Washington*. U.S. Geological Survey Professional Paper 1576. Washington: US Department of the Interior, US Geological Survey.
- Buehner, Ted. 2021. "Outdoor Tsunami Warning Sirens Coming to the North Sound." *Everett Post*, June 30, 2021. Everett Post. Edmonds, WA. <https://www.everettpost.com/press-releases/outdoor-tsunami-warning-sirens-coming-to-the-north-sound>. Archived at <https://web.archive.org/web/20220605012559/https://www.everettpost.com/press-releases/outdoor-tsunami-warning-sirens-coming-to-the-north-sound>.
- Busta, Hallie. 2016. "Post-Tsunami Sustainable Reconstruction Plan of Constitución." *Architecture Magazine*. January 13, 2016. https://www.architectmagazine.com/project-gallery/post-tsunami-sustainable-reconstruction-plan-of-constitucion_o. Archived at https://web.archive.org/web/20170810225511/http://www.architectmagazine.com/project-gallery/post-tsunami-sustainable-reconstruction-plan-of-constitucion_o,

- Callery, John. n.d. *Image of Beach, Washington: 91526266*. Photo. Dreamstime.com. Washington. Accessed May 18, 2022. <https://www.dreamstime.com/stock-photo-pacific-coast-washington-state-forest-meets-ocean-northern-image91526266>. Archived at <https://web.archive.org/web/20220605014704/https://www.dreamstime.com/stock-photo-pacific-coast-washington-state-forest-meets-ocean-northern-image91526266>.
- Cochard, Roland, Senaratne L. Ranamukhaarachchi, Ganesh P. Shivakoti, Oleg V. Shipin, Peter J. Edwards, and Klaus T. Seeland. 2008. "The 2004 Tsunami in Aceh and Southern Thailand: A Review on Coastal Ecosystems, Wave Hazards and Vulnerability." *Perspectives in Plant Ecology, Evolution and Systematics* 10 (1): 3–40. <https://doi.org/10.1016/j.ppees.2007.11.001>.
- Danielsen, Finn, Mikael K. Sorensen, Mette F. Olwig, Vaithilingam Selvam, Faizal Parish, Neil D. Burgess, Tetsuya Hiraishi, et al. 2005. "The Asian Tsunami: A Protective Role for Coastal Vegetation." *Science* 310 (5748): 643–44.
- Dengler, Lori, and Jane Preuss. 2003. "Mitigation Lessons from the July 17, 1998 Papua New Guinea Tsunami." *Pure and Applied Geophysics* 160 (10): 2001–31. <https://doi.org/10.1007/s00024-003-2417-x>.
- Design Work Underway for Shoalwater Tsunami Evacuation Tower*. 2019. Image. Chinook Observer. Tokeland, WA. https://www.chinookobserver.com/news/local/design-work-underway-for-shoalwater-tsunami-evacuation-tower/article_70dc7792-676f-11e9-af80-e39cec07a664.html. Archived at https://web.archive.org/web/20190501004947/https://www.chinookobserver.com/news/local/design-work-underway-for-shoalwater-tsunami-evacuation-tower/article_70dc7792-676f-11e9-af80-e39cec07a664.html.
- Diaz, Felipe. n.d. *Post-Tsunami Sustainable Reconstruction Plan of Constitución*. Photo. Architect Magazine. Constitución, Chile. Accessed May 17, 2022. https://www.architectmagazine.com/project-gallery/post-tsunami-sustainable-reconstruction-plan-of-constitucion_o. Archived at https://web.archive.org/web/20170810225511/http://www.architectmagazine.com/project-gallery/post-tsunami-sustainable-reconstruction-plan-of-constitucion_o.
- Eungard, Daniel W., Corina Forson, Timothy J. Walsh, Edison Gica, and Diego Arcas. 2018a. "Washington Geological Survey Map Series 2018-01." Washington Dept of Natural Resources. <https://www.dnr.wa.gov/programs-and-services/geology/geologic-hazards/geologic-hazard-maps#tsunami-inundation>. Archived at <https://web.archive.org/web/20220111210904/https://www.dnr.wa.gov/programs-and-services/geology/geologic-hazards/geologic-hazard-maps>.
- . 2018b. *Washington Geological Survey Map Series 2018-01: Map Sheet 3 of 5*. Map. WA DNR/NOAA. <https://www.dnr.wa.gov/programs-and-services/geology/geologic-hazards/geologic-hazard-maps#tsunami-inundation>. Archived at <https://web.archive.org/web/20220111210904/https://www.dnr.wa.gov/programs-and-services/geology/geologic-hazards/geologic-hazard-maps>.

- . 2018c. *Washington Geological Survey Map Series 2018-01: Map Sheet 5 of 6*. Map. WA DNR/NOAA. <https://www.dnr.wa.gov/programs-and-services/geology/geologic-hazards/geologic-hazard-maps#tsunami-inundation>. Archived at <https://web.archive.org/web/20220111210904/https://www.dnr.wa.gov/programs-and-services/geology/geologic-hazards/geologic-hazard-maps>.
- “Geologic Hazard Maps.” n.d. WA Dept of Natural Resources. Accessed June 4, 2022. <https://www.dnr.wa.gov/programs-and-services/geology/geologic-hazards/geologic-hazard-maps#tsunami-evacuation>. Archived at <https://web.archive.org/web/20220111210904/https://www.dnr.wa.gov/programs-and-services/geology/geologic-hazards/geologic-hazard-maps>.
- Goldfinger, Chris, C. Hans Nelson, and Joel E. Johnson. 2003. “Holocene Earthquake Records from the Cascadia Subduction Zone and Northern San Andreas Fault Based on Precise Dating of Offshore Turbidites.” *Annual Review of Earth and Planetary Sciences* 31: 555–78.
- Harrington, Constance A. n.d. “Red Alder.” USDA. Accessed May 17, 2022. https://www.srs.fs.usda.gov/pubs/misc/ag_654/volume_2/alnus/rubra.htm. Archived at https://web.archive.org/web/20211214112902/https://srs.fs.usda.gov/pubs/misc/ag_654/volume_2/alnus/rubra.htm.
- Harris, A.S. n.d. “Sitka Spruce.” USDA. Accessed May 17, 2022. https://www.srs.fs.usda.gov/pubs/misc/ag_654/volume_1/picea/sitchensis.htm. Archived at https://web.archive.org/web/20210902072733/https://srs.fs.usda.gov/pubs/misc/ag_654/volume_1/picea/sitchensis.htm.
- Heaton, Thomas H., and Stephen H. Hartzell. 1986. “Source Characteristics of Hypothetical Subduction Earthquakes in the Northwestern United States.” *Bulletin of the Seismological Society of America* 76 (3): 675–708. <https://doi.org/10.1785/BSSA0760030675>.
- . 1989. “Estimation of Strong Ground Motions from Hypothetical Earthquakes on the Cascadia Subduction Zone, Pacific Northwest.” *Pure and Applied Geophysics* 129 (1): 131–201. <https://doi.org/10.1007/BF00874626>.
- Heaton, Thomas H., and Hiroo Kanamori. 1984. “Seismic Potential Associated with Subduction in the Northwestern United States.” *Bulletin of the Seismological Society of America* 74 (3): 933–41. <https://doi.org/10.1785/BSSA0740030933>.
- Huang, Zhenhua, Yu Yao, Shawn Y. Sim, and Yao Yao. 2011. “Interaction of Solitary Waves with Emergent, Rigid Vegetation.” *Ocean Engineering* 38 (10): 1080–88. <https://doi.org/10.1016/j.oceaneng.2011.03.003>.
- Igarashi, Yoshiya, and Norio Tanaka. 2018. “Effectiveness of a Compound Defense System of Sea Embankment and Coastal Forest against a Tsunami.” *Ocean Engineering* 151 (March): 246–56. <https://doi.org/10.1016/j.oceaneng.2018.01.036>.

- limura, Kosuke, and Norio Tanaka. 2013. "Dangerous Zone Formation behind Finite-Length Coastal Forest for Tsunami Mitigation." *Journal of Earthquake and Tsunami* 07 (04): 1350034. <https://doi.org/10.1142/S1793431113500346>.
- limura, Kosuke, Norio Tanaka, Kenji Harada, and Katsutoshi Tanimoto. 2011. "Experimental Investigation for the Effects of Tree Arrangement in a Forest on Mitigating Tsunami." *34th IAHR Biennial Congress*, 1286–93.
- limura, Kosuke, Norio Tanaka, and Hirokazu Ikeda. 2013. "Effect of a Combined Position of Coastal Forest and Embankment on the Tree Breakage and Tsunami Mitigation." *Journal of Japan Society of Civil Engineers, Ser. B2 (Coastal Engineering)* 69 (2): I_401-I_405. https://doi.org/10.2208/kaigan.69.I_401.
- Indonesia's 'Green Belt' – Mangroves for Local and Global Benefits*. 2021. Photo. World Bank Group. Tarakan, Indonesia. <https://blogs.worldbank.org/eastasiapacific/indonesias-green-belt-mangroves-local-and-global-benefits>. Archived at <https://web.archive.org/web/20211111135237/https://blogs.worldbank.org/eastasiapacific/indonesias-green-belt-mangroves-local-and-global-benefits>.
- Irtem, Emel, Nuray Gedik, M. Sedat Kabdasli, and Nilay E. Yasa. 2009. "Coastal Forest Effects on Tsunami Run-up Heights." *Ocean Engineering* 36 (3): 313–20. <https://doi.org/10.1016/j.oceaneng.2008.11.007>.
- Ismail, H., A. K. Abd Wahab, and N. E. Alias. 2012. "Determination of Mangrove Forest Performance in Reducing Tsunami Run-up Using Physical Models." *Natural Hazards* 63 (2): 939–63. <https://doi.org/10.1007/s11069-012-0200-y>.
- Iverson, Alicia. 2015. *Cascadia Subduction Zone*. Map. Wikimedia Commons. https://commons.wikimedia.org/wiki/File:Cascadia_Subduction_Zone.jpg. Archived at https://web.archive.org/web/20190619225632/https://commons.wikimedia.org/wiki/File:Cascadia_Subduction_Zone.jpg.
- Jan. 26, 2022 Washington State Parks Regular Commission Work Session*. 2022. Video. WA State Parks and Recreation Commission. <https://www.youtube.com/watch?v=VgFaFT-Rl4I>. Archived at <https://web.archive.org/web/20220409222727/https://www.youtube.com/watch?v=VgFaFT-Rl4I>.
- Japan Earthquake and Tsunami of 2011*. 2011. Photo. Encyclopedia Britannica. Miyako, Japan. <https://www.britannica.com/event/Japan-earthquake-and-tsunami-of-2011#/media/1/1761942/264380>. Archived at <https://web.archive.org/web/20220529115424/https://www.britannica.com/event/Japan-earthquake-and-tsunami-of-2011>.
- Japan Earthquake of 2011*. n.d. Map. Encyclopedia Britannica. Accessed May 18, 2022. <https://www.britannica.com/event/Japan-earthquake-and-tsunami-of-2011#/media/1/1761942/154525>. Archived at <https://web.archive.org/web/20220529115424/https://www.britannica.com/event/Japan-earthquake-and-tsunami-of-2011>.

Japanese Ground Self-Defense Force, Ofunato, Iwate Prefecture, Japan. 2011. Photo. Encyclopedia Britannica. Ofunato, Japan. <https://www.britannica.com/event/Japan-earthquake-and-tsunami-of-2011#/media/1/1761942/154582>. Archived at <https://web.archive.org/web/20220529115424/https://www.britannica.com/event/Japan-earthquake-and-tsunami-of-2011>.

“JetStream Max: Cascadia Subduction Zone.” 2019. NOAA | NWS. August 13, 2019. https://www.weather.gov/jetstream/cascadia_max. Archived at https://web.archive.org/web/20211013031034/https://www.weather.gov/jetstream/cascadia_max.

Kahkonen, Satu, and André Rodrigues de Aquino. 2021. “Indonesia’s ‘Green Belt’ – Mangroves for Local and Global Benefits.” *World Bank Blogs* (blog). October 27, 2021. <https://blogs.worldbank.org/eastasiapacific/indonesias-green-belt-mangroves-local-and-global-benefits>. Archived at <https://web.archive.org/web/20211111135237/https://blogs.worldbank.org/eastasiapacific/indonesias-green-belt-mangroves-local-and-global-benefits>.

Kelsey, Harvey M., Robert C. Witter, and Eileen Hemphill-Haley. 2002. “Plate-Boundary Earthquakes and Tsunamis of the Past 5500 Yr, Sixes River Estuary, Southern Oregon.” *GSA Bulletin* 114 (3): 298–314. [https://doi.org/10.1130/0016-7606\(2002\)114<0298:PBEATO>2.0.CO;2](https://doi.org/10.1130/0016-7606(2002)114<0298:PBEATO>2.0.CO;2).

Kusumoto, Satoshi, Kentaro Imai, Aditya Riadi Gusman, and Kenji Satake. 2020. “Reduction Effect of Tsunami Sediment Transport by a Coastal Forest: Numerical Simulation of the 2011 Tohoku Tsunami on the Sendai Plain, Japan.” *Sedimentary Geology* 407 (September): 105740. <https://doi.org/10.1016/j.sedgeo.2020.105740>.

Kyung-Hoon, Kim. 2018a. *Seven Years After Tsunami, Japanese Live Uneasily with Seawalls*. Photo. Reuters. Yamada village, Iwate Prefecture, Japan. <https://www.reuters.com/article/us-japan-disaster-seawalls-idUSKCN1GL0DK>. Archived at <https://web.archive.org/web/20220515225443/https://www.reuters.com/article/us-japan-disaster-seawalls-idUSKCN1GL0DK>.

———. 2018b. *Seven Years After Tsunami, Japanese Live Uneasily with Seawalls*. Photo. Reuters. Taro town, Iwate Prefecture, Japan. <https://www.reuters.com/article/us-japan-disaster-seawalls-idUSKCN1GL0DK>. Archived at <https://web.archive.org/web/20220515225443/https://www.reuters.com/article/us-japan-disaster-seawalls-idUSKCN1GL0DK>.

———. 2018c. *Seven Years After Tsunami, Japanese Live Uneasily with Seawalls*. Photo. Reuters. Tanohata village, Iwate Prefecture, Japan. <https://www.reuters.com/article/us-japan-disaster-seawalls-idUSKCN1GL0DK>. Archived at <https://web.archive.org/web/20220515225443/https://www.reuters.com/article/us-japan-disaster-seawalls-idUSKCN1GL0DK>.

———. 2018d. “After the Tsunami: Japan’s Sea Walls – in Pictures.” *The Guardian*, March 9, 2018, sec. World news. <http://www.theguardian.com/world/gallery/2018/mar/09/after-the-tsunami-japan-sea-walls-in-pictures>. Archived at <https://web.archive.org/web/20220203194531/https://www.theguardian.com/world/gallery/2018/mar/09/after-the-tsunami-japan-sea-walls-in-pictures>.

- Lamontagne, Christian. 2016. *Morino Project*. Photo. PUR Projet. Japan. <https://www.purprojet.com/project/morino/>. Archived at <https://web.archive.org/web/20210422210928/https://www.purprojet.com/project/morino/>.
- Lunghino, Brent, Adrian F. Santiago Tate, Miho Mazereeuw, Abdul Muhari, Francis X. Giraldo, Simone Marras, and Jenny Suckale. 2020. "The Protective Benefits of Tsunami Mitigation Parks and Ramifications for Their Strategic Design." *Proceedings of the National Academy of Sciences* 117 (20): 10740–45. <https://doi.org/10.1073/pnas.1911857117>.
- Mapping a First Look at Tonga's Devastation After the Volcano Eruption*. 2022. Map. The New York Times. <https://www.nytimes.com/interactive/2022/01/18/world/australia/tonga-map.html>. Archived at <https://web.archive.org/web/20220530191009/https://www.nytimes.com/interactive/2022/01/18/world/australia/tonga-map.html>.
- Mascarenhas, Antonio, and Seelam Jayakumar. 2008. "An Environmental Perspective of the Post-Tsunami Scenario along the Coast of Tamil Nadu, India: Role of Sand Dunes and Forests." *Journal of Environmental Management, Environmental Aspects of the Indian Ocean Tsunami Recovery*, 89 (1): 24–34. <https://doi.org/10.1016/j.jenvman.2007.01.053>.
- McCurry, Justin. 2011. "Japan Upgrades Nuclear Crisis to Same Level as Chernobyl." *The Guardian*, April 12, 2011, sec. World news. <https://www.theguardian.com/world/2011/apr/12/japan-nuclear-crisis-chernobyl-severity-level1>. Archived at <https://web.archive.org/web/20220421012529/https://www.theguardian.com/world/2011/apr/12/japan-nuclear-crisis-chernobyl-severity-level1>.
- Minore, Don. n.d. "Western Red Cedar." USDA. Accessed May 17, 2022. https://www.srs.fs.usda.gov/pubs/misc/ag_654/volume_1/thuja/plicata.htm. Archived at https://web.archive.org/web/20210902072834/https://srs.fs.usda.gov/pubs/misc/ag_654/volume_1/thuja/plicata.htm.
- Minore, Don, and John C. Zasada. n.d. "Big Leaf Maple." USDA. Accessed May 17, 2022. https://www.srs.fs.usda.gov/pubs/misc/ag_654/volume_2/acer/macrophyllum.htm. Archived at https://web.archive.org/web/20220120013743/https://www.srs.fs.usda.gov/pubs/misc/ag_654/volume_2/acer/macrophyllum.htm.
- "Morino Project." 2016. PUR Projet. Accessed May 17, 2022. <https://www.purprojet.com/project/morino/>. Archived at <https://web.archive.org/web/20210422210928/https://www.purprojet.com/project/morino/>.
- Morino Project*. 2016. Image. PUR Projet. <https://www.purprojet.com/project/morino/>. Archived at <https://web.archive.org/web/20210422210928/https://www.purprojet.com/project/morino/>.
- Nandasena, N. A. K., Yasushi Sasaki, and Norio Tanaka. 2012. "Modeling Field Observations of the 2011 Great East Japan Tsunami: Efficacy of Artificial and Natural Structures on Tsunami Mitigation." *Coastal Engineering* 67 (September): 1–13. <https://doi.org/10.1016/j.coastaleng.2012.03.009>.

- Nateghi, Roshanak, Jeremy D. Bricker, Seth D. Guikema, and Akane Bessho. 2016. "Statistical Analysis of the Effectiveness of Seawalls and Coastal Forests in Mitigating Tsunami Impacts in Iwate and Miyagi Prefectures." *PLoS ONE* 11 (8): e0158375–e0158375. <https://doi.org/10.1371/journal.pone.0158375>.
- Noguchi, Hironori, Hajime Sato, Hiroyuki Torita, K Masaka, T Abe, K Kimura, and T Sakamoto. 2012. "Numerical Simulation of the Effect of Inundation Flow Caused by the 2011 Tohoku Earthquake Tsunami on the Pinus Thunbergii Coastal Forest: A Case Study of Misawa City of the Aomori Prefecture (in Japanese with English Abstract)." *Journal of Japanese Society of Coastal Forests* 11 (2): 47–51.
- Nomura, Reika, Shinsuke Takase, Shuji Moriguchi, Kenjiro Terada, and Randall J. LeVeque. 2021. "Multiscale Evaluation Method of the Drag Effect on Shallow Water Flow through Coastal Forests Based on 3D Numerical Simulations." *International Journal for Numerical Methods in Fluids* 94 (1): 32–58. <https://doi.org/10.1002/flid.5046>.
- "On This Day: 2011 Tohoku Earthquake and Tsunami." 2021. NOAA | NCEI. March 11, 2021. <http://www.ncei.noaa.gov/news/day-2011-japan-earthquake-and-tsunami>. Archived at <https://web.archive.org/web/20220430104045/https://www.ncei.noaa.gov/news/day-2011-japan-earthquake-and-tsunami>.
- Outdoor Tsunami Warning Sirens Coming to the North Sound*. 2021. Photo. Everett Post. Edmonds, WA. <https://www.everettpost.com/press-releases/outdoor-tsunami-warning-sirens-coming-to-the-north-sound>. Archived at <https://web.archive.org/web/20220605012559/https://www.everettpost.com/press-releases/outdoor-tsunami-warning-sirens-coming-to-the-north-sound>.
- Packee, E. C. n.d. "Western Hemlock." USDA. Accessed May 17, 2022. https://www.srs.fs.usda.gov/pubs/misc/ag_654/volume_1/tsuga/heterophylla.htm. Archived at https://web.archive.org/web/20220330060724/https://www.srs.fs.usda.gov/pubs/misc/ag_654/volume_1/tsuga/heterophylla.htm.
- Pasha, Ghufuran Ahmed, and Norio Tanaka. 2016. "Effectiveness of Finite Length Inland Forest in Trapping Tsunami-Borne Wood Debris." *Journal of Earthquake and Tsunami* 10 (04): 1650008. <https://doi.org/10.1142/S1793431116500081>.
- Peterson, Curt D., Harry M. Jol, Sandy Vanderburgh, James B. Phipps, David Percy, and Guy Gelfenbaum. 2010. "Dating of Late Holocene Beach Shoreline Positions by Regional Correlation of Coseismic Retreat Events in the Columbia River Littoral Cell, USA." *Marine Geology*, Large-scale coastal change in the Columbia River littoral cell, 273 (1): 44–61. <https://doi.org/10.1016/j.margeo.2010.02.003>.
- Post-Tsunami Sustainable Reconstruction Plan of Constitución*. 2010. Photo. Architect Magazine. Constitución, Chile. https://www.architectmagazine.com/project-gallery/post-tsunami-sustainable-reconstruction-plan-of-constitucion_o. Archived at https://web.archive.org/web/20170810225511/http://www.architectmagazine.com/project-gallery/post-tsunami-sustainable-reconstruction-plan-of-constitucion_o.

- “Preparation and Evacuation.” n.d. WA State DNR. Accessed May 31, 2022. <https://www.dnr.wa.gov/programs-and-services/geology/geologic-hazards/Tsunamis#preparation-and-evacuation.4>. Archived at <https://web.archive.org/web/20220323234610/https://www.dnr.wa.gov/programs-and-services/geology/geologic-hazards/Tsunamis#preparation-and-evacuation.4>.
- Pringle, Russell. 1986. “Soil Survey of Grays Harbor County Area, Pacific County, and Wahkiakum County, Washington.” USDA. https://www.nrcs.usda.gov/Internet/FSE_MANUSCRIPTS/washington/WA627/0/wa627_text.pdf.
- “Project Safe Haven: Tsunami Vertical Evacuation Systems on Washington State’s Pacific Coast.” 2021. FEMA. February 11, 2021. <https://www.fema.gov/node/465491>. Archived at <https://web.archive.org/web/20210413024737/https://www.fema.gov/node/465491>.
- “Resource Issues: Coastal Armoring and Erosion.” 2019. NOAA | Monterey Bay National Marine Sanctuary. December 9, 2019. <https://montereybay.noaa.gov/resourcepro/resmanissues/coastal.html>. Archived at <https://web.archive.org/web/20220517145009/https://montereybay.noaa.gov/resourcepro/resmanissues/coastal.html>.
- Samarakoon, M. B., Norio Tanaka, and Kosuke Iimura. 2013. “Improvement of Effectiveness of Existing Casuarina Equisetifolia Forests in Mitigating Tsunami Damage.” *Journal of Environmental Management* 114 (January): 105–14. <https://doi.org/10.1016/j.jenvman.2012.10.050>.
- Satake, Kenji, K. Shimazaki, Y. Tsuji, and K. Ueda. 1996. “Time and Size of a Giant Earthquake in Cascadia Inferred from Japanese Tsunami Records of January 1700.” *Nature* 379 (6562): 246–49.
- Satake, Kenji, Kelin Wang, and Brian F. Atwater. 2003. “Fault Slip and Seismic Moment of the 1700 Cascadia Earthquake Inferred from Japanese Tsunami Descriptions.” *Journal of Geophysical Research: Solid Earth* 108 (B11). <https://doi.org/10.1029/2003JB002521>.
- Sato, Hajime, Hiroyuki Torita, K Masaka, T Abe, Hironori Noguchi, K Kimura, and T Sakamoto. 2012. “Relationship between Treefall Damage and Forest Structure of Pinus Thunbergii Coastal Forest by the 2011 Tohoku Earthquake Tsunami Disaster: An Example of Misawa City of Aomori Prefecture (in Japanese with English Abstract).” *Journal of Japanese Society of Coastal Forests* 11 (2): 41–45.
- Sea Wall Coastal Defense*. 2008. Photo. PhotoEverywhere.co.uk. Wales, United Kingdom. https://photoeverywhere.co.uk/britain/welshcoast/slides/sea_defenses0151.htm. Archived at https://web.archive.org/web/20210511125641/https://photoeverywhere.co.uk/britain/welshcoast/slides/sea_defenses0151.htm.
- Sharma, Manas, and Simon Scarr. 2022. “How Big Was the Tonga Eruption?” *Reuters*, January 21, 2022. <https://graphics.reuters.com/TONGA-VOLCANO/lgpdwjqbvo/>. Archived at <https://web.archive.org/web/20220501055247/https://graphics.reuters.com/TONGA-VOLCANO/lgpdwjqbvo/>.

- Shimbun, Mainichi. 2021. *When the Japan Tsunami Struck*. Photo. Reuters. Miyako, Japan. <https://www.reuters.com/news/picture/when-the-japan-tsunami-struck-idUSRTR2JR13>. Archived at <https://web.archive.org/web/20220530180024/https://www.reuters.com/news/picture/when-the-japan-tsunami-struck-idUSRTR2JR13>.
- Sue. 2017. Photo: *Where Forest Meets Ocean on the Northern Oregon Coast*. Photo. ExplorerSue.com. Oregon. <https://www.explorersue.com/forest-meets-ocean-northern-oregon-coast/>. Archived at <https://web.archive.org/web/20170102054436/http://www.explorersue.com/forest-meets-ocean-northern-oregon-coast/>.
- Suppasri, Anawat, Erick Mas, Ingrid Charvet, Rashmin Gunasekera, Kentaro Imai, Yo Fukutani, Yoshi Abe, and Fumihiko Imamura. 2013. "Building Damage Characteristics Based on Surveyed Data and Fragility Curves of the 2011 Great East Japan Tsunami." *Natural Hazards* 66 (2): 319–41. <https://doi.org/10.1007/s11069-012-0487-8>.
- Tanaka, Norio. 2009. "Vegetation Bioshields for Tsunami Mitigation: Review of Effectiveness, Limitations, Construction, and Sustainable Management." *Landscape and Ecological Engineering* 5 (1): 71–79. <http://dx.doi.org/10.1007/s11355-008-0058-z>.
- . 2012. "Effectiveness and Limitations of Coastal Forest in Large Tsunami: Conditions of Japanese Pine Trees on Coastal Sand Dunes in Tsunami Caused by Great East Japan Earthquake." *Journal of Japan Society of Civil Engineers*, Ser. B1 (Hydraulic Engineering) 68 (4): II_7-II_15. https://doi.org/10.2208/jscejhe.68.II_7.
- Tanaka, Norio, N. Nandasena, K. Jinadasa, Y. Sasaki, K. Tanimoto, and M. Mowjood. 2009. "Developing Effective Vegetation Bioshield for Tsunami Protection." *Civil Engineering & Environmental Systems* 26 (2): 163–80. <https://doi.org/10.1080/10286600802435850>.
- Tanaka, Norio, Yu Niwata, Hajime Sato, Hiroyuki Torita, and Hironori Noguchi. 2015. "High-precision Tsunami Simulation Method Considering the Difference in Breaking and Overturning Phenomenon by Stand Structure of Coastal Trees Applicable to Coastal Forest Management." *Journal of Japan Society of Civil Engineers*, Ser. B2 (Coastal Engineering) 71 (2): I_307-I_312. https://doi.org/10.2208/kaigan.71.I_307.
- Tanaka, Norio, and Kazuyoshi Ogino. 2017. "Comparison of Reduction of Tsunami Fluid Force and Additional Force Due to Impact and Accumulation after Collision of Tsunami-Produced Driftwood from a Coastal Forest with Houses during the Great East Japan Tsunami." *Landscape and Ecological Engineering* 13 (2): 287–304. <http://dx.doi.org/10.1007/s11355-016-0321-7>.
- Tanaka, Norio, and Aki Onai. 2017. "Mitigation of Destructive Fluid Force on Buildings Due to Trapping of Floating Debris by Coastal Forest during the Great East Japan Tsunami." *Landscape & Ecological Engineering* 13 (1): 131–44. <https://doi.org/10.1007/s11355-016-0308-4>.

- Tanaka, Norio, Yasushi Sasaki, M. I. M. Mowjood, KBSN Jinadasa, and Samang Homchuen. 2007. "Coastal Vegetation Structures and Their Functions in Tsunami Protection: Experience of the Recent Indian Ocean Tsunami." *Landscape and Ecological Engineering* 3 (1): 33–45. <http://dx.doi.org/10.1007/s11355-006-0013-9>.
- Tanaka, Norio, Hajime Sato, Yoshiya Igarashi, Yuya Kimiwada, and Hiroyuki Torita. 2018. "Effective Tree Distribution and Stand Structures in a Forest for Tsunami Mitigation Considering the Different Tree-Breaking Patterns of Tree Species." *Journal of Environmental Management* 223 (October): 925–35. <https://doi.org/10.1016/j.jenvman.2018.07.006>.
- Tanaka, Norio, Junji Yagisawa, and Satoshi Yasuda. 2013. "Breaking Pattern and Critical Breaking Condition of Japanese Pine Trees on Coastal Sand Dunes in Huge Tsunami Caused by Great East Japan Earthquake." *Natural Hazards* 65 (1): 423–42. <https://doi.org/10.1007/s11069-012-0373-4>.
- Tanaka, Norio, Satoshi Yasuda, Kosuke Iimura, and Junji Yagisawa. 2014. "Combined Effects of Coastal Forest and Sea Embankment on Reducing the Washout Region of Houses in the Great East Japan Tsunami." *Journal of Hydro-Environment Research* 8 (3): 270–80. <https://doi.org/10.1016/j.jher.2013.10.001>.
- Tanimoto, Katsutoshi, Norio Tanaka, N. A. K. Nandasena, Kosuke Iimura, and Takashi Shimizu. 2007. "Numerical Simulation of Tsunami Prevention by Coastal Forest with Several Species of Tropical Tree." *Proceedings of Coastal Engineering, Jsce* 54: 1381–85. <https://doi.org/10.2208/proce1989.54.1381>.
- Tappin, David R., Hannah M. Evans, Colm J. Jordan, Bruce Richmond, Daisuke Sugawara, and Kazuhisa Goto. 2012. "Coastal Changes in the Sendai Area from the Impact of the 2011 Tohoku-Oki Tsunami: Interpretations of Time Series Satellite Images, Helicopter-Borne Video Footage and Field Observations." *Sedimentary Geology, The 2011 Tohoku-oki tsunami*, 282 (December): 151–74. <https://doi.org/10.1016/j.sedgeo.2012.09.011>.
- Tariq, Kamran, Ghufuran Ahmed Pasha, Norio Tanaka, Usman Ghani, and Afzal Ahmed. 2021. "Development of Ecosystem-Based Flood Mitigation Approach – Investigations by Experiments and Numerical Simulation." *Water and Environment Journal* 35 (2): 685–703. <https://doi.org/10.1111/wej.12662>.
- Taumoefolau, Faka'iloatonga. 2022. *Tsunami Hits Tonga After Underwater Volcano Erupts in South Pacific*. Photo. CNN. Nuku'alofa, Tonga. https://www.cnn.com/asia/live-news/tonga-tsunami-warning-volcano-eruption/h_1c7b3c8ec74c66faf19f97ebe4b57ee3. Archived at <https://web.archive.org/web/20220201231154/https://www.cnn.com/asia/live-news/tonga-tsunami-warning-volcano-eruption/index.html>.
- Tauranga Sea Wall Rock Revetment – TerraTex K Geotextile*. 2018. Photo. Cirtex Industries. Tauranga, New Zealand. <https://cirtexcivil.co.nz/case-studies/tauranga-sea-wall-rock-revetment-terratex-k-geotextile/>. Archived at <https://web.archive.org/web/20220217190920/https://cirtexcivil.co.nz/case-studies/tauranga-sea-wall-rock-revetment-terratex-k-geotextile/>.

- Thuy, Nguyen Ba, Katsutoshi Tanimoto, and Norio Tanaka. 2010. "Force Due to Tsunami Runup around a Coastal Forest with a Gap — Experiments and Numerical Simulations." *Science of Tsunami Hazards* 29 (2): 44–69.
- Thuy, Nguyen Ba, Katsutoshi Tanimoto, Norio Tanaka, Kenji Harada, and Kosuke Iimura. 2009. "Effect of Open Gap in Coastal Forest on Tsunami Run-up—Investigations by Experiment and Numerical Simulation." *Ocean Engineering* 36 (15): 1258–69. <https://doi.org/10.1016/j.oceaneng.2009.07.006>.
- Tognin, Davide, Paolo Peruzzo, Francesca De Serio, Mouldi Ben Meftah, Luca Carniello, Andrea Defina, and Michele Mossa. 2019. "Experimental Setup and Measuring System to Study Solitary Wave Interaction with Rigid Emergent Vegetation." *Sensors* 19 (8): 1787. <https://doi.org/10.3390/s19081787>.
- Tomizawa, Sadatsugu. 2011. *Every Minute Counts*. Photo. Getty Images via New Scientist. Minamisoma, Japan. <https://www.newscientist.com/article/2129373-seabed-seismic-sensors-would-have-cut-2011-japan-tsunami-toll/>. Archived at <https://web.archive.org/web/20220414161825/https://www.newscientist.com/article/2129373-seabed-seismic-sensors-would-have-cut-2011-japan-tsunami-toll/>.
- "Tonga Volcanic Eruption and Tsunami, January 15, 2022." 2022. NOAA | NCEI. 2022. <https://ngdc.noaa.gov/hazard/15jan2022.html>. Archived at <https://web.archive.org/web/20220305170320/https://ngdc.noaa.gov/hazard/15jan2022.html>.
- "Trees and Shrubs for Riparian Plantings." 2010. USDA Natural Resources Conservation Service. https://www.nrcs.usda.gov/Internet/FSE_PLANTMATERIALS/publications/wapmstn13160.pdf.
- Tsai, Ching-Piao, Ying-Chi Chen, Tri Octaviani Sihombing, and Chang Lin. 2017. "Simulations of Moving Effect of Coastal Vegetation on Tsunami Damping." *Natural Hazards and Earth System Sciences* 17 (5): 693–693.
- "Tsunami." n.d. Washington State Military Dept. Accessed May 31, 2022. <https://mil.wa.gov/tsunami>. Archived at <https://web.archive.org/web/20220313045255/https://mil.wa.gov/tsunami>.
- "Tsunami Frequently Asked Questions." n.d. NOAA/NWS. Accessed May 17, 2022. <https://tsunami-cp.ncep.noaa.gov/?page=tsunamiFAQ>. Archived at <https://web.archive.org/web/20210307152535/https://tsunami-cp.ncep.noaa.gov/?page=tsunamiFAQ>.
- Tsunami Models Underestimated Shockwave from Tonga Eruption*. 2022a. Image. Reuters. <https://www.reuters.com/world/asia-pacific/tsunami-models-underestimated-shockwave-tonga-eruption-2022-01-28/>. Archived at <https://web.archive.org/web/20220517202106/https://www.reuters.com/world/asia-pacific/tsunami-models-underestimated-shockwave-tonga-eruption-2022-01-28/>.

- . 2022b. Photo. Reuters. Tongatapu, Tonga. <https://www.reuters.com/world/asia-pacific/tsunami-models-underestimated-shockwave-tonga-eruption-2022-01-28/>. Archived at <https://web.archive.org/web/20220517202106/https://www.reuters.com/world/asia-pacific/tsunami-models-underestimated-shockwave-tonga-eruption-2022-01-28/>.
- Tsunami Wave Height Model*. 2011. Image. Encyclopedia Britannica. <https://www.britannica.com/event/Japan-earthquake-and-tsunami-of-2011#/media/1/1761942/154566>. Archived at <https://web.archive.org/web/20220529115424/https://www.britannica.com/event/Japan-earthquake-and-tsunami-of-2011>.
- Tsunamis | Preparation and Evacuation | Vertical Evacuation*. n.d.-a Photo. WA DNR. Westport, WA. Accessed May 18, 2022. <https://www.dnr.wa.gov/programs-and-services/geology/geologic-hazards/tsunamis/#preparation-and-evacuation.6>. Archived at <https://web.archive.org/web/20220323234610/https://www.dnr.wa.gov/programs-and-services/geology/geologic-hazards/Tsunamis>.
- . n.d.-b Image. WA DNR. Accessed May 18, 2022. <https://www.dnr.wa.gov/programs-and-services/geology/geologic-hazards/tsunamis/#preparation-and-evacuation.6>. Archived at <https://web.archive.org/web/20220323234610/https://www.dnr.wa.gov/programs-and-services/geology/geologic-hazards/Tsunamis>.
- Udo, Keiko, Daisuke Sugawara, Hitoshi Tanaka, Kentaro Imai, and Akira Mano. 2012. "Impact of the 2011 Tohoku Earthquake and Tsunami on Beach Morphology along the Northern Sendai Coast." *Coastal Engineering Journal* 54 (01): 1250009. <https://doi.org/10.1142/S057856341250009X>.
- "U.S. Tsunami Warning System." 2016. NOAA. April 19, 2016. <https://www.noaa.gov/explainers/us-tsunami-warning-system>. Archived at <https://web.archive.org/web/20220215102808/https://www.noaa.gov/explainers/us-tsunami-warning-system>.
- Walton, Maureen A.L., Lydia M. Staisch, Tina Dura, Jessie K. Pearl, Brian Sherrod, Joan Gomberg, Simon Engelhart, et al. 2021. "Toward an Integrative Geological and Geophysical View of Cascadia Subduction Zone Earthquakes." *Annual Review of Earth and Planetary Sciences* 49 (1): 367–98. <https://doi.org/10.1146/annurev-earth-071620-065605>.
- Washington State Major Land Resource Areas (MLRA) Map*. 2010. Map. USDA Natural Resources Conservation Service. https://www.nrcs.usda.gov/Internet/FSE_PLANTMATERIALS/publications/wapmstn13160.pdf.
- "Westport Light State Park." n.d. Washington State Parks. Accessed May 17, 2022. <https://parks.wa.gov/284/Westport-Light>. Archived at <https://web.archive.org/web/20220510233428/https://parks.wa.gov/284/Westport-Light>.
- Westport Tsunami Evacuation Walk Times*. 2019. Map. WA DNR. <https://www.dnr.wa.gov/programs-and-services/geology/geologic-hazards/geologic-hazard-maps#tsunami-evacuation>. Archived at <https://web.archive.org/web/20220111210904/https://www.dnr.wa.gov/programs-and-services/geology/geologic-hazards/geologic-hazard-maps>.

When the Japan Tsunami Struck. 2021a. Photo. Reuters. Fukushima Prefecture, Japan. <https://www.reuters.com/news/picture/when-the-japan-tsunami-struck-idUSRTR2JR13>. Archived at <https://web.archive.org/web/20220530180024/https://www.reuters.com/news/picture/when-the-japan-tsunami-struck-idUSRTR2JR13>.

———. 2021b. Photo. Reuters. Iwanuma, Japan. <https://www.reuters.com/news/picture/when-the-japan-tsunami-struck-idUSRTR2JR13>. Archived at <https://web.archive.org/web/20220530180024/https://www.reuters.com/news/picture/when-the-japan-tsunami-struck-idUSRTR2JR13>.

Witter, Robert C., Harvey M. Kelsey, and Eileen Hemphill-Haley. 2003. "Great Cascadia Earthquakes and Tsunamis of the Past 6700 Years, Coquille River Estuary, Southern Coastal Oregon." *GSA Bulletin* 115 (10): 1289–1306. <https://doi.org/10.1130/B25189.1>.

Witter, Robert C., Yinglong J. Zhang, Kelin Wang, George R. Priest, Chris Goldfinger, Laura Stimely, John T. English, and Paul A. Ferro. 2013. "Simulated Tsunami Inundation for a Range of Cascadia Megathrust Earthquake Scenarios at Bandon, Oregon, USA." *Geosphere* 9 (6): 1783–1803. <https://doi.org/10.1130/GES00899.1>.

Wreckage From Japan Earthquake and Tsunami of 2011. 2011. Photo. Encyclopedia Britannica. Ofunato, Japan. <https://www.britannica.com/event/Japan-earthquake-and-tsunami-of-2011#/media/1/1761942/154568>. Archived at <https://web.archive.org/web/20220529115424/https://www.britannica.com/event/Japan-earthquake-and-tsunami-of-2011>.